



저작자표시-비영리-변경금지 2.0 대한민국

이용자는 아래의 조건을 따르는 경우에 한하여 자유롭게

- 이 저작물을 복제, 배포, 전송, 전시, 공연 및 방송할 수 있습니다.

다음과 같은 조건을 따라야 합니다:



저작자표시. 귀하는 원저작자를 표시하여야 합니다.



비영리. 귀하는 이 저작물을 영리 목적으로 이용할 수 없습니다.



변경금지. 귀하는 이 저작물을 개작, 변형 또는 가공할 수 없습니다.

- 귀하는, 이 저작물의 재이용이나 배포의 경우, 이 저작물에 적용된 이용허락조건을 명확하게 나타내어야 합니다.
- 저작권자로부터 별도의 허가를 받으면 이러한 조건들은 적용되지 않습니다.

저작권법에 따른 이용자의 권리는 위의 내용에 의하여 영향을 받지 않습니다.

이것은 [이용허락규약\(Legal Code\)](#)을 이해하기 쉽게 요약한 것입니다.

[Disclaimer](#)

의학박사 학위논문

Development and Validation of
Assessment Tools Using Robotic and
Virtual Reality Technologies in Stroke
Rehabilitation

로봇 및 가상현실 기술을 이용한
뇌졸중 재활 평가도구의 개발 및
검증

2016년 8월

서울대학교 대학원

의학과 재활의학 전공

김 원 석

A thesis of the Degree of Doctor of Philosophy

로봇 및 가상현실 기술을 이용한
뇌졸중 재활 평가도구의 개발 및
검증

Development and Validation of
Assessment Tools Using Robotic and
Virtual Reality Technologies in Stroke
Rehabilitation

August 2016

The Department of Rehabilitation Medicine,
Seoul National University
College of Medicine
Won-Seok Kim

로봇 및 가상현실 기술을 이용한 뇌졸중 재활 평가도구의 개발 및 검증

지도교수 백남종

이 논문을 의학박사 학위논문으로 제출함
2016 년 4 월

서울대학교 대학원
의학과 재활의학 전공
김 원 석

김원석 의 의학박사 학위논문을 인준함
2016 년 6 월

위원장	<u>김 성 완</u>	(인)
부위원장	<u>백 남 종</u>	(인)
위 원	<u>정 선 근</u>	(인)
위 원	<u>박 형 순</u>	(인)
위 원	<u>조 규 진</u>	(인)

Abstract

Development and Validation of Assessment Tools Using Robotic and Virtual Reality Technologies in Stroke Rehabilitation

Won-Seok Kim

Department of Medicine, Rehabilitation Medicine

The Graduate School

Seoul National University

Introduction: Stroke is a leading cause of disabilities worldwide. It is important to recover the functional independence of patients after stroke to decrease socioeconomic burdens. Rehabilitation is necessary as an integral part of stroke care in modern medicine. Among many components in stroke rehabilitation, assessment is important for planning current function-based rehabilitation and monitoring the recovery. Recently, technologies such as robotics and virtual realities are actively applied to stroke rehabilitation. These two technologies could be used to objectively assess rehabilitation interventions, increase the reliability of preexisting assessment tools, monitor patient's function remotely, and assess their functional independence more quantitatively. The objective of this study was to determine the usefulness of

robotics and virtual realities-based technologies for assessments in stroke rehabilitation.

Methods: Four experiments were performed in this study. In the first experiment, robotic elbow device was used to investigate the differences between isotonic and isokinetic elbow extension exercises. Nine stroke patients performed three sets of isotonic elbow extensions at 30% of their maximal voluntary isometric torque followed by three sets of maximal isokinetic elbow extensions. The mean angular velocity and total amount of work were standardized for each matched set in two strengthening modes. All exercises were performed using 1-DoF planner robot to regulate the exact resistive torque and speed. Surface electromyographic activities of eight muscles in the hemiplegic shoulder and elbow were recorded. Normalized root mean square (RMS) values and co-contraction index (CCI) were used for the analysis.

Robotic elbow device was used to increase the reliability of modified Tardieu Scale (MTS) in the second experiment. Two independent raters measured the catch angle three times per assessor. The isokinetic robotic device was then used to measure the catch angle at velocity of 200 degree/s. Inter- and intra-rater reliabilities were calculated both manually and with robotic assessments. Box and Block Test (BBT), a conventional assessment tool, is simple and easy to apply. Its usefulness in stroke rehabilitation has been demonstrated in previous studies. In the third study, we developed a virtual BBT (VBBT) and investigated its validity for stroke patients. Using a conventional depth-sensing camera, we developed an assessment system for hand, finger, and grasping. The BBT used for grasping ability test in hospitals was virtualized

with the same setting. VBBT was validated in patients with mild hemiplegia after stroke.

In the fourth experiment, we developed a Fugl-Meyer Assessment (FMA) tool using Kinect (Microsoft, USA) and validated it for hemiplegic stroke patients. A total of 41 patients with hemiplegic stroke were enrolled. Thirteen of 33 items were selected for upper extremity motor FMA. One occupational therapist assessed motor FMA while upper extremity motion was recorded with Kinect. FMA score was calculated using principal component analysis and artificial neural network learning from the saved motion data. The degree of jerky motion was transformed to jerky scores. Prediction accuracy of each of the 13 items was determined. Correlations between real FMA scores and scores using Kinect were analyzed.

Results: The isokinetic mode was shown to activate agonists of elbow extension more efficiently than the isotonic mode (normalized RMS for pooled triceps: 96.0 ± 17.0 (2nd) and 87.8 ± 14.4 (3rd) in isokinetic vs. 80.9 ± 11.0 (2nd) and 81.6 ± 12.4 (3rd) in isotonic contraction, $F[1,8] = 11.168$; $P = 0.010$) without increasing the co-contraction of muscle pairs, implicating spasticity or synergy. The test-retest and inter-rater reliabilities for measuring catch angle (R1) using isokinetic robotic devices were extremely excellent. The number of blocks moved in the BBT showed strong correlation with the VBBT in the non-hemiplegic side (Pearson's $r = 0.904$, $P = 0.001$) and the hemiplegic side (Pearson's $r = 0.788$, $P = 0.012$). With regard to prediction of FMA using Kinect, the prediction accuracies ranged from 65% to 87% in each item and more than 70% for 9 items. For the summed score of the 13 items, real FMA scores were highly correlated with scores obtained using

Kinect (Pearson's $r=0.873$, $P<0.0001$). Total upper extremity scores (66 in full score) were also highly correlated with scores using Kinect (26 in full score) (Pearson's $r=0.799$, $P<0.0001$). Log transformed jerky scores in the hemiplegic side (1.81 ± 0.76) were significantly higher than those in the non-hemiplegic side (1.21 ± 0.43). Log transformed jerky scores showed significant negative correlations with Brunnstrom stage (3 to 6; Spearman correlation coefficient = -0.387 , $P=0.046$).

Conclusions: Robotic device is useful for comparing different modes of rehabilitation in more standardized manner to increase the reliability of preexisting assessment tool. Virtual reality technology with depth-sensing camera can be used as a useful and inexpensive tele-assessment tool for measuring post-stroke motor function in a home-based setting to provide quantitative measures of motion for stroke patients. However, assessment tools used in our study have some limitations. Further efforts are needed to increase the fidelity of rehabilitation care by combining different current technologies or developing novel technologies.

Keywords: Robot, Virtual reality, Hemiplegia, Stroke, Depth-sensing camera, Assessment, Rehabilitation

Student Number: 2012-30491

Contents

Abstract	i
Contents	v
List of tables	vi
List of figures	vii
List of abbreviations	ix
Introduction	1
Materials and Methods.....	3
Experiment 1.....	4
Experiment 2.....	17
Experiment 3.....	21
Experiment 4.....	31
Results.....	38
Experiment 1.....	38
Experiment 2.....	42
Experiment 3.....	46
Experiment 4.....	51
Discussion	57
Conclusion	69
References	70
Abstract in Korean	80

List of tables

Table 1. Baseline characteristics of the subjects	11
Table 2. Baseline characteristics of subjects (n=18)	18
Table 3. Test-retest (intra-rater) reliability results for the passive range of motion (R2), angle of catch (R1), Tardieu Scores (R2-R1) data measured with goniometry, isokinetic robotic devices and robotic devices with manual motion	43
Table 4. Inter-rater reliability results for the passive range of motion (R2), angle of catch (R1), Tardieu Scores (R2-R1) data measured with goniometry, isokinetic robotic devices and robotic devices with manual motion	45
Table 5. Baseline characteristics of the subjects	47
Table 6. Results of the real and virtual box and block test (BBT).....	48
Table 7. Baseline characteristics of patients (n=41)	52

List of figures

Figure 1. Overview of this study with four experiments	3
Figure 2. Total experiment platform	5
Figure 3. 1-DoF planner robot device	6
Figure 4. Diagram of the control system	8
Figure 5. The experimental setup	10
Figure 6. Box and Block Test in the virtual environment	21
Figure 7. Sequence of Virtual Box and Block Test	25
Figure 8. Hand Skeleton	27
Figure 9. Motion data recording program	32
Figure 10. RMS values for elbow extensors (A) and elbow flexors (B) according to the modes of exercise (isotonic vs. isokinetic) and set orders (second and third)	39
Figure 11. Normalized co-contraction index from the pairs of the lateral head of the triceps/long head of biceps and the posterior deltoid/lateral head of the triceps according to the modes of exercise (isotonic vs. isokinetic) and set orders (second and third)	41
Figure 12. Correlations between the numbers of box moved in the real and those in the virtual BBT in the non-hemiplegic side (A), and in the hemiplegic side (B), and the correlation between the percent ratios [(the number of boxes moved by the hemiplegic side)/(the number of boxes	

moved by the normal side) * 100 %] in the real and those in the virtual	
BBT (C)	50
Figure 13. Prediction accuracies (%) of Fugl-Meyer assessment (FMA)	
scores using Kinect for real FMA scores in each item	53
Figure 14. Correlation data	55
Figure 15. Correlation between log (jerky score) and Brunnstrom arm	
stage (3 to 6) in the hemiplegic upper extremity (n=27) (Spearman	
correlation coefficient = -0.387, $P=0.046$)	56

List of abbreviations

BBT = Box and Block Test

FMA = Fugl-Meyer Assessment

MVIC = Maximum Voluntary Isometric Contraction

RMS = Root Mean Square

CCI = Co-contraction Index

EMG = Electromyography

MEA = Maximum EMG Activation

ANOVA = Analysis of Variance

ROM = Range of Motion

Modified Tardieu Scale = MTS

ICC = Intraclass Correlation Coefficient

SEM = Standard Errors of Measurements

VBBT = Virtual Box and Block Test

HCS = Hand Close State

GGD = Grasping Gesture Detected

ANN = Artificial Neural Network

INTRODUCTION

Stroke is the leading cause of disability in the world[1]. Motor impairment such as hemiparesis is one of the most common disabilities after stroke. It brings great burden to families and society[2]. Therefore, great efforts are needed to reduce motor impairment after stroke. Rehabilitation has been reported to be effective in reducing motor impairment after stroke. However, there is no one single aid that can greatly improve motor recovery after stroke. Traditional rehabilitation has some shortcomings to overcome. First, the assessment and treatment methods during rehabilitation are not well standardized. They depend on medical staff's experiences. Second, accessibility to traditional rehabilitation can be limited to stroke patients who have some disabilities. Only about 30% of stroke survivors in the United States receive outpatient stroke rehabilitation, which is lower than the expected percentage considering the clinical practice guideline[3]. This may be associated with barriers such as expensive rehabilitation costs, long distance from home to the rehabilitation facility and limited use of transportation due to disabilities[3]. Furthermore, rehabilitation facilities are limited in developing countries. Therefore, the use of outpatient rehabilitation is likely very low in developing countries[4].

Technologies such as robotics and virtual realities are recently introduced to the rehabilitation field to solve the problems in traditional stroke rehabilitation[5, 6]. Robotic stroke rehabilitation has shown some promise in clinical research and its application in the clinical field is increasing[7, 8]. In addition to robotic treatment, assessment using robot can also enhance the

reliability and validity of traditional assessment, thus enhancing the quality and standardization of practice. In addition, it can provide better prognostic factor for recovery[9, 10]. More precise and reliable assessment can also reduce the sample size for clinical trials in the rehabilitation field[11]. Quantitative measurements and simulation of standardized motion for stroke patients can be used to investigate the effect of different rehabilitation strategies on stroke patients.

Virtual reality technologies are also widely tried as alternative rehabilitation tools in stroke patients. Virtual reality technologies can simulate standard motor rehabilitation. They can be applied in home-based rehabilitation setting without direct supervision of a therapist. Among many components in home-based rehabilitation systems, objective functional assessment is important to plan current function-based rehabilitation and monitor the recovery. A depth-sensing camera, such as Kinect (Microsoft, USA), can detect joint movement three-dimensionally[12]. It may be used to assess the motor function of stroke patients. In addition, real-time joint tracking with Kinect makes motion analysis possible[13, 14]. It can provide quantitative results for movement quality, which is difficult when manual assessment tool is used[13, 14]. In addition, Kinect is a relatively cheap sensor without needing additional hardware except a computer to acquire motion data for the assessment of motor function in a virtual reality environment.

Therefore, in this study, a robotic device was used to control and measure the elbow motion of stroke patients and virtual reality technologies with a depth-sensing camera were used. Their usefulness for stroke patients in the field of clinical rehabilitation was determined.

MATERIALS AND METHODS

Four experiments were performed in this study. First, robotic elbow devices were developed and applied to stroke patients. Differences between isotonic and isokinetic strengthening exercises in stroke patients with spastic elbow and reliability of robot-assisted modified Tardieu scale, one of the measurements for spasticity, were determined. Second, virtual box and block test (BBT) and Fugl-Meyer Assessment (FMA) were developed using depth sensing camera and validated for the assessment of upper extremity function in stroke patients. An overview of this study with the four experiments is shown in Figure 1. All procedures described in this section were approved by the Institutional Review Board of Seoul National University Bundang Hospital.

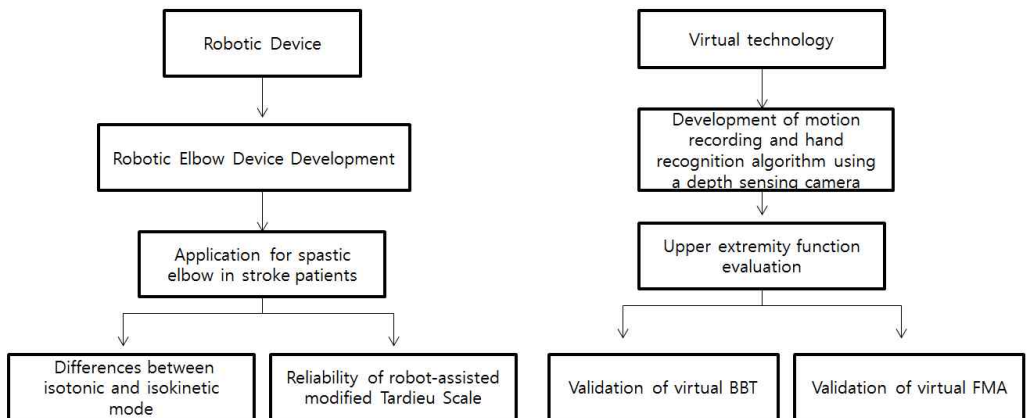


Figure 1. Overview of this study with four experiments

Experiment 1. Electromyographic analysis of upper limb muscles during standardized isotonic and isokinetic robotic exercise

1-1. Subjects

Inclusion criteria were as follows: (1) unilateral hemiparesis in the upper extremity caused by unilateral first-ever stroke, (2) 20 years or older, (3) elbow joint spasticity in the range of one plus to three in the modified Ashworth scale in the hemiparetic arm, (4) voluntary elbow extension strength of three or above in the hemiparetic arm as measured by the manual muscle test proposed by Medical Research Council, (5) no previous disease affecting the function of the hemiparetic arm, except for stroke itself (6) free of cognitive, language, visuospatial or attention deficits that would prevent subjects from following the experimental procedures, and (7) free of medical conditions which would cause hemodynamic instability. Patients were recruited from June 2012 to September 2012. The subjects were inpatients or outpatients with stroke in one department of rehabilitation medicine of a tertiary hospital. One physiatrist is affiliated with the department of rehabilitation medicine screened the patients, and total of nine patients who met the above-mentioned criteria and provided their written consent were enrolled in this study. This research was approved by the local institutional review board and was conducted in accordance with the regulatory standards of Good Clinical Practice and the Declaration of Helsinki (World Medical Association Declaration of Helsinki: Ethical Principles for Medical Research Involving

Human Subjects, 2008).

1-2. System and devices

For the experiment, we designed a customized experimental platform. The experimental platform consists of 5 parts as shown in the Figure 2: an exoskeleton part, a control unit part, a measurement unit, a base platform part and a chair.

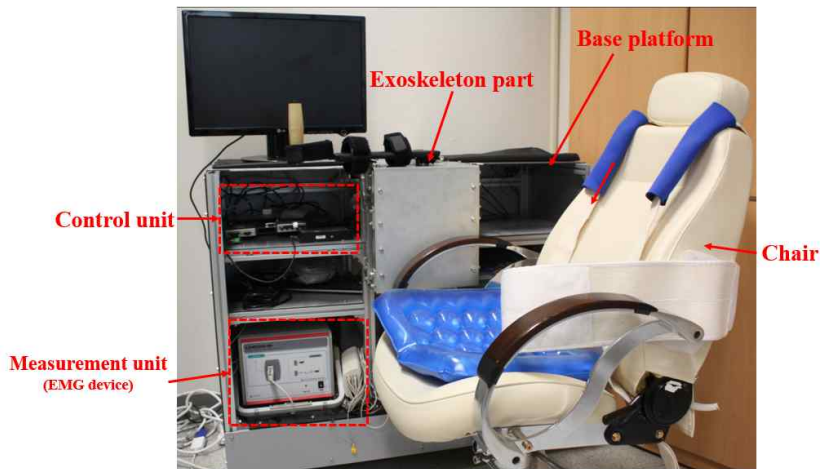


Figure 2. Total experiment platform[15]

The exoskeleton part is a 1-Dof planar robot; Figure 3 shows the details of the exoskeleton part. The exoskeleton part uses a brushed DC motor (RE-50, Maxon, Switzerland) with a power rating of 200 W, nominal speed of 5680 rpm and a continuous torque of 405 mNm. This motor is used in combination with a gearhead with a reduction ratio of 66:1. The reduction ratio is small enough to make the exoskeleton as back-drivable as possible, thus the robot can produce a nominal speed of 86rpm and a continuous torque of 26.7Nm. The arm manipulandum is made as lightweight as possible in order to

minimize its inertial effects. A torque sensor (TRT-500, 500 inch lbs, Transducer Techniques, USA) is mounted between the manipulandum and the motor to measure the interaction torque between the exoskeleton and the user. The encoder (HEDL 5540, Maxon, Switzerland) is attached on the motor to measure angle and angular velocity.

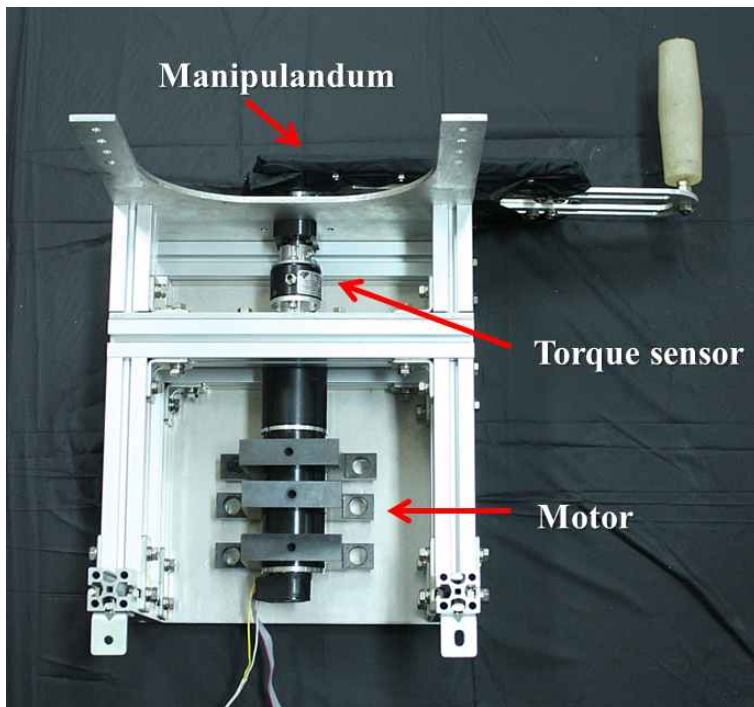


Figure 3. 1-DoF planner robot device[15]

Figure 4 shows the diagram of the devices and system for our experiment. The control unit consists of PC, NI Single-Board RIO (sbRio-9632, National Instruments, Austin, TX) and a motor driver (EPOS2 70/10, Maxon, Switzerland). The PC is used as a control tower. It provides GUI to control the robot and to store robot data (angle, angular velocity and interaction torque) as time advances. NI Single-Board RIO is used as a main controller. The main

control algorithm is implemented in NI Single-Board RIO with a sampling rate of 0.1 kHz. The algorithm calculates the desired motion, transmits the results to the motor driver, collects motor data and sends them to the PC. The motor driver is a low level controller and it is connected with NI Single-Board RIO by the CAN BUS. The motor driver receives angle and angular velocity data from the motor and sends the data to the main controller. And by applying appropriate current to motor, the motor driver provides various control modes: position control mode, velocity control mode and current control mode. The position control mode has been used to implement isometric exercise, the velocity control mode to isokinetic exercise and the current control mode to isotonic exercise. The measurement unit is an eight-channel EMG system (Laxtha Inc., Daejeon, Korea). This EMG device was used to collect raw surface EMG signals to directly measure muscle activation. Output from the EMG system was directly linked to the PC, and raw data were monitored and collected at a sampling rate of 1024Hz. The base part is the main platform. It contains a control unit, a measurement unit and powers for the other components and the exoskeleton part mounted on the base platform. The chair part has shoulder straps and an abdominal strap in order to restrict torso movement, and the height of the chair is adjustable to let the subject's shoulder and the robot manipulandum lie in the same horizontal plane.

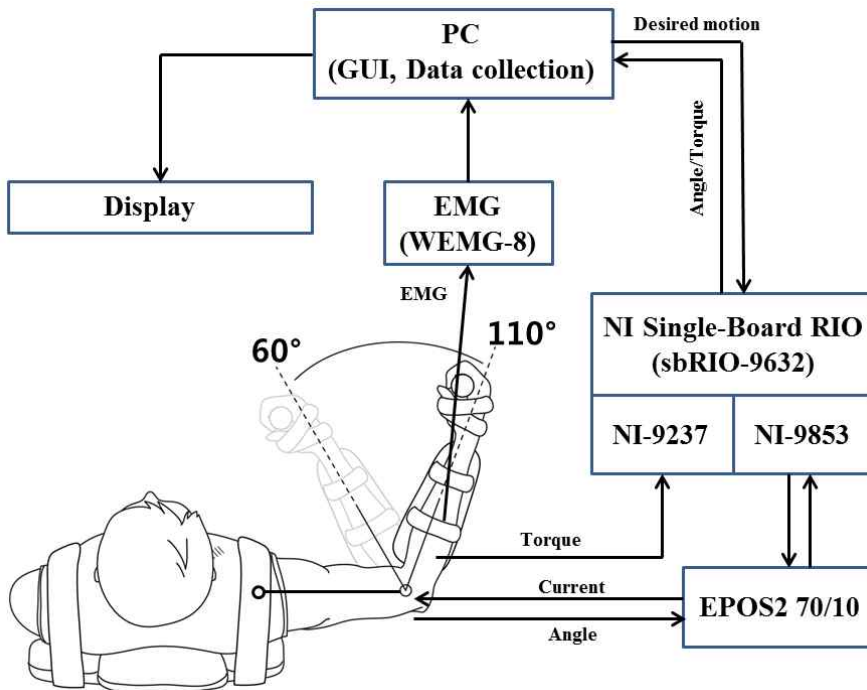


Figure 4. Diagram of the control system[15]

1-3. Experimental design

The experiment was designed to compare isotonic exercise and isokinetic exercise during elbow extension. The experimental protocol suggested by Remaud was used with modifications to compare the isotonic and the isokinetic exercise with standardization of mean angular velocity and total amount of work[16]. The experiment was divided into three sessions: setup, familiarization and actual test.

In the setup session, Brunnstrom and Fugl-Meyer Assessment (FMA) scale in the affected arm were checked. After that, surface electrodes (1.8 × 1.2 mm Ag–AgCl, Bioprotech Inc., Wonju, Korea) were attached on the following

muscles in the patient's hemiplegic upper extremity based on the "Surface EMG for Non-Invasive Assessment of Muscles (SENIAM)"[17]: anterior, middle and posterior deltoid, biceps short and long head, triceps long and lateral head and brachioradialis. One reference electrode was attached at the backside of neck.

After EMG electrodes were attached, the maximum voluntary isometric contraction (MVIC) of each muscle was performed to measure maximum EMG value. First, MVIC of shoulder and forearm muscles (anterior, middle and posterior deltoid and brachioradialis) was performed[18]. In the anatomical position of the hemiparetic upper extremity, three 5-second MVIC were performed while an experienced physiatrist blocked the shoulder from moving. In detail, the physiatrist stabilized the shoulder with one hand and the upper arm with the other hand while the patient was asked to exert maximum voluntary force in three directions; flexion, extension and abduction. 30-second rest period between trial and 2-minute rest period between each action were given. EMG activities were measured during MVIC of each muscle.

Before MVIC of upper arm muscles (biceps short and long head, triceps long and lateral head), subjects were set to experimental posture. Trunk of subject was restricted by shoulder and abdominal straps that attached to the chair and the height of the chair was adjusted to let the patient's shoulder and the robot lie in the same horizontal plane. The shoulder of the subject was abducted 90 degrees, forearm was in the neutral position and elbow was positioned at 90 degrees in the horizontal plane. The rotation axis of the robot was aligned to the anatomical axis of the elbow as shown in Figure 5. Forearm was fastened to the manipulandum using straps. Elbow angle of 90 degrees (with 180

degrees for full extension) was selected because it is known that the maximum torques of the elbow can be obtained around this angle[19].



Figure 5. The experimental setup[15]

Following the posture setting, MVIC of the upper arm muscles was assessed[20]. Three sets of 5-second elbow extension and flexion were performed with the same rest periods as the shoulder and forearm MVIC assessment. In addition to EMG activities, torques were measured during MVIC of the upper arm muscle (Figure 4).

In the familiarization session, subjects were asked to try both isotonic and isokinetic exercise. Resistive torque during isotonic elbow extension was set at 30% of the maximal elbow extension torque of each subject from the setup session. Several elbow isotonic extensions from 60 to 110 degree were tried. In cases the subjects cannot extend the elbow from 60 to 110 degrees during the isotonic mode, the range was adjusted (Table 1). After deciding the angle, several isotonic elbow extensions were performed. Next, several isokinetic elbow extensions with the same range and mean velocity of the previous isotonic session were performed.

Table 1. Baseline characteristics of the subjects

Patient No.	Age, years	Gender	Stroke onset to test, days	Stroke type	Hemiplegic side	MAS in hemiplegic arm		Brunnstrom stage in arm	FMA in U/E	Muscle strength in elbow		Tested elbow Range of motion, degree
						Elbow extensor	Elbow flexor			Elbow extensor	Elbow flexor	
1	29	F	1768	Ischemic	Left	3	3	3	34	4	4	60-110
2	80	M	60	Ischemic	Left	1+	1+	3	34	3	3	60-110
3	89	M	92	Ischemic	Right	2	2	4	47	3	3	50-80
4	47	F	1093	hemorrhagic	Right	3	3	3	23	3	3	60-100
5	46	M	1205	Ischemic	Right	3	3	4	38	3	3	60-100
6	60	M	1985	Ischemic	Left	3	3	3	30	4	4	60-110
7	63	F	80	hemorrhagic	Right	1+	1+	5	57	4	4	60-110
8	44	M	17	Ischemic	Right	1+	1+	4	49	3	3	60-90
9	47	M	15	hemorrhagic	Right	2	2	5	60	3	3	60-110

MAS: Modified Ashworth Sacle, FMA: Fugl-Meyer assessment, U/E: Upper extremity

Before actual test session, the subjects took a 10-minute rest period. Resistive torque and range of exercise were set using the same parameters determined in the familiarization session. Firstly, in the actual test session, the subjects performed three sets of six isotonic elbow extensions with a 2-minute rest period between the sets. During the isotonic elbow extension, angle, angular velocity and external torque were measured by the robot and mean angular velocity and total work done by the subjects were calculated for each exercise sets using external torque and angular velocity. After 10 minutes of rest period, the subjects performed standardized three sets of isokinetic elbow extension with the same rest period with isotonic elbow extensions. During the familiarization session, mean velocity of the isotonic extension session of each set was used as moving velocity of each isokinetic extension set. Total work done by the subjects was also calculated using the same method with the isotonic extension and each set of the isokinetic extension continued until the work reached the value of the matched isotonic extension set. No resistive torque was applied during reciprocal elbow flexion for both exercise modes. The detailed methods of standardization of isokinetic sets to the corresponding isotonic sets were described elsewhere[16]. EMG of the 8 muscles was measured during the only elbow extension contraction to verify the influence of spasticity and synergism during both the elbow effort exercises.

Immediately after completing the three sets of each isotonic and isokinetic sessions, the 15-point Borg scale was used to evaluate the degree of subjective muscle fatigue in the affected upper extremity[21]. A numeric rating scale (NRS) for pain ranging from 0 to 10 was used in the affected upper extremity before and after each isotonic and isokinetic session[22].

1-4. EMG data analysis

All data were processed by analysis software: TeleScan (Laxtha Inc., Daejeon, Korea) and MATLAB (Mathworks Inc., USA). Normalized root mean square (NRMS) EMG and co-contraction index (CCI) were calculated to identify the influence of the exercise for all 8 target muscles (anterior, middle and posterior deltoid, biceps short and long head, triceps long and lateral head and brachioradialis).

Before calculating the NRMS EMG and the CCI, all raw EMG data were pre-processed. The EMG data were corrected for DC bias removal and band-pass filtered from 10 to 450 Hz. After that, the processed EMG data was synchronized with the robot data (angle, angular velocity and torque). To synchronize data from two different devices (EMG and PC), trigger signals were made on each device. Trigger signals were activated before MVIC of upper arm muscle measurements, all data were realigned as the trigger signal point was regarded as 0 sec.

To calculate the NRMS EMG, maximum EMG activation (MEA) of each muscle and root mean square (RMS) EMG of each exercise set are needed. MEA was calculated from MVIC experiment data of 8 target muscles. MEA was calculated according to the following steps[16]:

- A. Calculate the moving RMS of the isometric EMG data; each data was averaged from ± 50 numbers of data.
- B. Find peak values from the moving RMS results of each muscle.
- C. Calculate MEA of each muscle by averaging the data of ± 100 ms of the peak moving RMS value.

RMS EMG was calculated from isotonic and isokinetic exercise results. To

regulate the experimental conditions of isotonic and isokinetic exercise equally, only EMG data of the predetermined ROM of extension phase were analyzed. RMS EMG was calculated according to following steps:

- A. Using the robot angle data, extract time data when the robot angle exists between the predetermined angle range of extension phase
- B. Extract EMG data that correspond to the time data of step A from the prior processed EMG data.
- C. Calculate RMS from the results of step B for each exercise set.

After calculating MEA and RMS EMG, the NRMS EMG was calculated by normalizing the RMS EMG results with MEA of each muscle.

The CCI was used to analyze co-contraction and synergy patterns of the subjects. The CCI equation was design based on the studies performed by Frost et al.[23] and Falconer[24, 25].

To calculate the CCI, at first, pre-processed EMG data of two muscles were full-wave rectified and similar with RMS EMG calculation only EMG data of the predetermined ROM of extension phase were used to CCI calculation. Then CCI was calculated using following equation (1):

$$CCI = \frac{2 \cdot IEMG_{overlap}}{IEMG_{total}} \times 100 \quad \dots\dots\dots \text{Equation (1)}$$

where $IEMG_{overlap}$ is the overlap area of the two muscles EMG activity which is calculated by using the following equation (2):

$$IEMG_{overlap} = \int \min(EMG_1, EMG_2) dt \quad \dots\dots\dots \text{Equation (2)}$$

$IEMG_{total}$ is used to normalize the $IEMG_{overlap}$ value. $IEMG_{total}$ is the sum of the integrated EMG of each muscle and is calculated using the following

equation (3):

$$IEMG_{total} = \int (EMG_1 + EMG_2) dt \quad \dots\dots\dots \text{Equation (3)}$$

To analyze all co-contraction and synergy patterns of the hemiplegic subjects, CCI of all possible muscle pairs (total 28 pairs of 8 muscles) were calculated.

1-5. Statistical analysis

The EMG data of the 8 muscles during only elbow extension contraction were used for analysis and only the data of the second and third isotonic and isokinetic sets were used for analysis. Two-way repeated measures ANOVA (mode (isotonic vs. isokinetic) x set order (second and third sets in each mode)) for two controlled parameters (mean angular velocity and total external amount of work realized) and repetition numbers of elbow extensions were used to see if the standardization was well performed and if the repetition numbers of elbow extension were different between two contraction exercises under the same work and angular velocity.

Two way repeated measures ANOVA (mode x series) for the normalized RMS values of eight muscles to see if which contraction exercise can more efficiently induce the contraction of the agonists during the elbow extension.

Two way repeated measures ANOVA (mode x series) for the normalized CCIs for each selected muscle pair were used to analyze if there is any differences in spasticity or synergy according to the mode of contraction exercises.

Mann-Whitney U test for the Borg scale was used to compare the level of fatigue after completing the elbow extension exercises between two

contraction exercises. Two-way repeated measures ANOVA (mode x time (pre- and post-session of each exercise mode)) for NRS were used to analyze the differences in pain of the affected upper extremity after completing each contraction exercise.

For repeated measures ANOVA, the Greenhouse-Geisser correction was used if the sphericity assumption was not met in Mauchly's test. Overall significant differences were determined by a two-tailed $P < 0.05$.

Experiment 2. Reliability of robotic device assisted modified Tardieu Scale measurements

2-1. Subjects

Patients were recruited from May 2015 to December 2015. These subjects were inpatients or outpatients with stroke from four rehabilitation hospitals. Inclusion criteria were as follows: (1) hemiparesis in the upper extremity caused by stroke, (2) 20years or older, (3) elbow joint spasticity in the range of one to three in the modified Ashworth scale in the hemiparetic arm, (4) no previous disease affecting the function of the hemiparetic arm except for stroke itself, (5) free of cognitive, language, visuospatial, or attention deficits that could prevent subjects from following experimental procedures, and (6) free of medical conditions that could cause hemodynamic instability. One physiatrist affiliated with the Department of Rehabilitation Medicine screened these patients. A total of 18 patients who met the above-mentioned criteria and provided their written consent were enrolled in this study. This research was approved by the local Institutional Review Board. It was conducted in accordance with the regulatory standards of Good Clinical Practice and the Declaration of Helsinki (World Medical Association Declaration of Helsinki: Ethical Principles for Medical Research Involving Human Subjects, 2008). Baseline characteristics of subjects are summarized in Table 2.

Table 2. Baseline characteristics of subjects (n=18)

Variable	Result
Age, years, mean (SD)	53.5 (12.7)
Gender, n (%)	
Men	14 (77.8)
Women	4 (22.2)
Hemiplegic side, n (%)	
Right	10 (55.6)
Left	8 (44.4)
Stroke type, n (%)	
Ischemic	12 (66.7)
Hemorrhagic	6 (33.3)
Stroke lesion, n (%)	
Cortical	5 (27.8)
Subcortical	13 (72.2)
Brunnstrom stage, median (IQR)	
Arm	4 (1)
Hand	3 (1)
Leg	4 (1)
Muscle Power, median (IQR)	
Elbow flexor	4 (2)
Elbow extensor	4 (1)
Modified Ashworth Scale, Elbow flexor	
1	6 (33.3)
1+	5 (27.8)
2	6 (33.3)
3	1 (5.6)

2-2. Experimental design

Patients sat on a chair comfortably with hemiparetic arm positioned in anatomical position. Two raters assessed the modified Tardieu Scale according to Boyd and Graham's method[26]. Rater 1 was a physiatrist with 10 years of experience in modified Tardieu Scale. Rater 2 is an occupational therapist

with 4-years of experience in MTS. To measure R2 (angle during passive motion) and R1 (catch of angle during fast movement), elbow was moved from maximal flexion (0 degrees) manually by a rater. For slow trials, a rater extended the elbow with a velocity below 5 degrees per second to measure the passive range of motion (ROM). The same rater who moved the patient's arm measured the angle with a goniometer. For fast trials, velocity was chosen to reach the terminal ROM within one second and the word brief "one" was used to meet this criteria[27]. After feeling the angle of catch, that angle was measured by the same rater. Raters were instructed not to change the position of elbow after feeling the catch and adjusting the position of elbow to that position. Raters were not allowed to see the angle in the goniometer before deciding the final position of elbow which the rater felt the catch. Each rater measured R2 and R1 three times. Raters were blinded to the angle measured by each other. The order of rater was randomized. Three minutes of interval was given between two raters' assessments.

After the manual MTS measurements in the shoulder neutral position, five minutes of rest was given. This experiment process was repeated with 90 degree of shoulder abduction and forearm neutral position.

After a rest of 10 minutes, the robotic device was applied to the subject. The shoulder of the subject was abducted 90 degrees. The forearm was in the neutral position. The elbow was positioned at 90 degrees in the horizontal plane. The rotation axis of the robot was aligned to the anatomical axis of the elbow as shown in Figure 5. Forearm was fastened to the manipulandum using straps. One rater set up this posture. The elbow was extended from maximal flexed position with isokinetic velocity of 200 degrees/sec by the

robotic elbow device. Resistive torque was measured during isokinetic movement. The movement was stopped if the torque reached 0.6 Nm. That angle was recorded as a catch angle. After that, the rater extended subject's elbow manually by applying the robotic device with a velocity of "one". The angle of catch (R1) was retrospectively decided using the resistive torque for each rater during manual measurements with shoulder at 90 degree abduction. These were repeated three times for each rater. The order of rater was randomized. There was a 3-minute-interval between two raters' assessments.

2-3. Statistical analysis

Data of angles (R1 and R2) measured during the second and third tests were used for statistical analysis. Paired sample t-tests were used to test differences between the second and third tests in each rater or between two raters. P-values less than 0.05 were considered as statistically significant. Test-retest and inter-rater reliabilities of goniometry with shoulder neutral position or goniometry with shoulder of 90 degree abduction, isokinetic robotic device, or robotic device with manual motion were computed with intraclass correlation coefficient (ICC). Reliability was considered as extremely excellent for values exceeding 0.90, excellent for values from 0.75 to 0.90, fair to good for values between 0.40 and 0.75, and poor for values less than 0.40[28]. The standard error of measurements (SEM) was calculated to determine the error component of the variance. From the SEM, the smallest detectable difference (SDD) was calculated for test-retest data. Statistical analysis was performed using SPSS version 18.0 (SPSS, Chicago, IL, USA).

Experiment 3. Upper limb function assessment using virtual Box and Block Test (VBBT) in stroke

3-1. VBBT environment

In order to detect the user's hand, a Kinect is held by a frame at 1m from the table to enable a clear view of the hand. The virtual space configuring the VBBT is visualized in the monitor under the frame as shown in Figure 6.

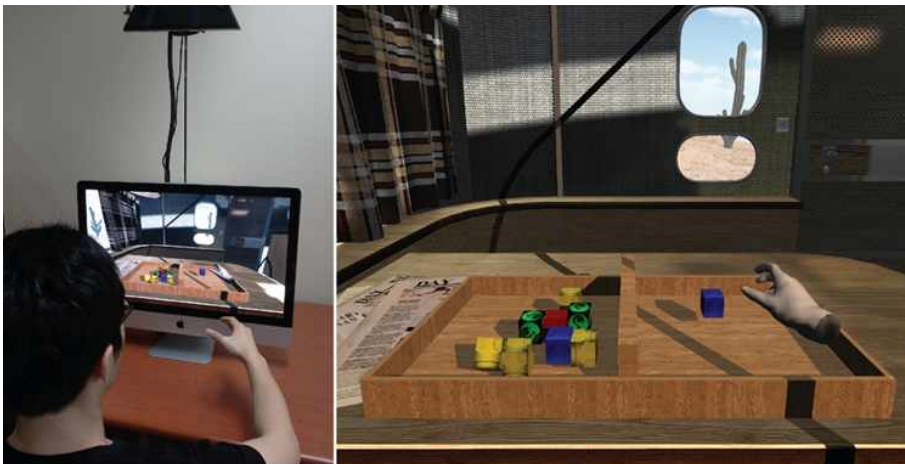


Figure 6. Box and Block Test in the virtual environment[29].

A Microsoft Kinect is held on viewing the left. The system recognizes the user's hand and finger grasping actions and calculates their grasping and box carrying abilities.

The area in front of the monitor is the space for the user's hand interaction. In the area, the user's hand movement is reflected by the virtual hand. The user moves his/her hands with the visual feedback.

The VBBT program is developed in the Unity game engine

(<http://unity3d.com/unity>). The Unity game engine is a game development IDE recently favored by diverse developers, from those in the gaming industry to those in academia. It facilitates rendering high-end real-time graphics, simulates virtual physics, and utilizes various programming languages (C#, JavaScript, Boo) while making it easy to design and implement GUI (Graphical User Interface). As mentioned above, the BBT is an assessment that utilizes estimates of the box-grasping and -carrying actions of patients. In order to visualize the assessment, the recognition of fine hand movement is required. We used an open source library called Threegear Systems (<http://threegear.com/technology.html>). Threegear Systems provides the transmitter, which transmits dummy information about the hands by UDP communication, such as the transformation information of the hand skeletons (16 joints), the data on the estimated hand geometry (vertices' positions), and the recognition results of the hand gestures. This information is parsed for each dataset in the VBBT program.

As mentioned above, we developed a program that, like the BBT, assesses a patient's movement ability when grasping and carrying items. However, ours does so automatically and in the virtual world. In the virtual space, the VBBT set is composed of two compartments filled with boxes and a barrier. The VBBT has the following characteristics that distinguish it from the BBT.

Every object without a virtual hand has physical properties (e.g., mass, collision, friction) for a realistic visualization. Contrary to real hands, virtual hands cannot be directly affected by physical feedback like tactile and force feedback during contact and collision with other virtual objects without hand-held devices. If a virtual hand has physical properties without physical

feedback, it moves freely with no reaction force, which can affect the false physical activities of other objects.

In the BBT, a patient has to move boxes in one compartment to the other compartment. On the other hand, in the case of the VBBT, a box is created in each trial in one virtual compartment. When the patient puts the box in the other virtual compartment, another box is automatically created in the first compartment. This is done to effectively measure the grasping action of the target box and to avoid obstructing the view of the target box by collisions with other boxes. As it lacks physical properties, the virtual hand might grasp another hidden box instead of the target box in the filled compartment. It is inappropriate for testing hand positioning. Thus, in summary, our VBBT system created only one target box in the first compartment in order to evaluate patients' hand-positioning ability.

Hand modes, visual effects, and scoring rules are embodied in the system to simulate the therapist of the BBT in the virtual world. A left- or right-hand mode for the assessment is chosen when the program starts. Only the corresponding hand is visualized in the display. As with the BBT, the compartment on the same side as the chosen hand is the first compartment where boxes are placed. A target box is created in the first compartment when a previous box is carried over to the second compartment. A user can only grasp a target box, and he/she is notified of this by a color-change signal. To assess the patient's carrying ability with the box-grasping motion, successful box carrying is recognized only when a user drops a box from a position under the height of the barrier. A correctly carried box count is visualized in the display. Boxes put in the second compartment are stacked up to show the

number of attempts of the user.

3-2. Grasp a box method

The hand recognition result, which the hand recognition software of Threegear transmits in the VBBT program, is composed of three key–value pairs. Keys are skeleton, vertices, and posture, which correspond to the values of hand skeleton, hand vertices for rendering, and detected hand posture, respectively. This hand recognition result is parsed by each key. The hand skeleton dataset and the hand posture information are used for more accurate grasping detection. The hand mesh is made up of hand vertices. The target box has three states to determine the movement types: Hand Close State (HCS), Grasping Gesture Detected (GGD), and Hand Following State (HFS). The HCS is activated when the virtual hand is close to the box and the box changes color to notify the user (Figure 7A). The ‘close’ state means the intersection of an invisible finger-sized sphere and the box. The sphere is located in the center position of the metacarpal base joint of the thumb, index, and middle finger, similar to a realistic grasping area. The GGD is activated when the user uses a grasping gesture and maintains grasping posture (Figure 7B). Simultaneously activating the HCS and GGD activates the HFS, and the box follows the hand (Figure 7C). Not maintaining the grasping posture in the HFS deactivates the GGD, causing the HFS to also deactivate (Figure 7D). Objects without the virtual hand are affected by physics. Therefore, when the box grasped by the hand is carried, if the box contacts the barrier at the center of the two compartments, the system forces the deactivation of the GGD and HFS, and the box is dropped due to a gravity effect.

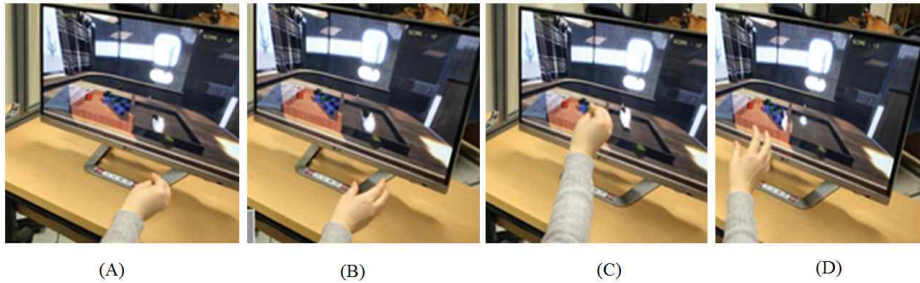


Figure 7. Sequence of Virtual Box and Block Test[29].

In right hand test, user locate their hand on a box in right compartment (A), grasp the box (B), move on holding the box (C), and drop the box in left compartment (D).

3-3. Grab algorithm for accurate grasp detection

Hand postures provided by Threegear System are useful for the interaction and control of the computer or the virtual world, similar to a keyboard or mouse. However, the recognition of hand poses is limited, especially the recognition of the pinch pose by the Threegear System, which is similar to the grasping pose in the VBBT. In order to detect the pinch pose, the depth camera must view the contact between the thumb and index fingertips. However, it is impossible for the depth camera to detect every contact, because the grasping pose varies in many situations and can be occluded. The user could be forced to pose such that the contact of the thumb and index fingertips is well captured. However, a forced pose to enable detection is not only difficult for some users, such as the stroke patients in our experiments, but it could also result in a negative effect. In order to detect the grasping even if the contact was not captured by the depth camera, we used the hand joint angle data of the thumb, index, and middle fingers rather than the contact of

the thumb and index finger. For more robust recognition, we used a classification method called Linear Discriminant Analysis (LDA), which is used in statistics, pattern recognition, and machine learning to find linear combinations of features. This combination might be used as a linear classifier. We used finger joint angles for to finding detect the grasping motion. θ has 9nine elements as shown below: Equation (4)

$$\theta = (\theta_{02}, \theta_{01}, \theta_{00}, \theta_{12}, \theta_{11}, \theta_{10}, \theta_{22}, \theta_{21}, \theta_{20})^T \dots\dots\dots \text{Equation (4)}$$

Each θ_j is made from the cosine of two knuckle vectors (equation (5)).

$$\theta_j = \cos^{-1}(\mathbf{F}_{ij} - \mathbf{F}_{ij-1}) \cdot (\mathbf{F}_{ij+1} - \mathbf{F}_{ij}) \dots\dots\dots \text{Equation (5)}$$

, where i is 0, 1, 2 and j is 1, 2. When j is 0, the angle is

$$\theta_0 = \cos^{-1}(\mathbf{F}_{i0} - \mathbf{W}) \cdot (\mathbf{F}_{i1} - \mathbf{F}_{i0}) \dots\dots\dots \text{Equation (6)}$$

\mathbf{F}_{ij} is a recognized finger position in Figure 8.

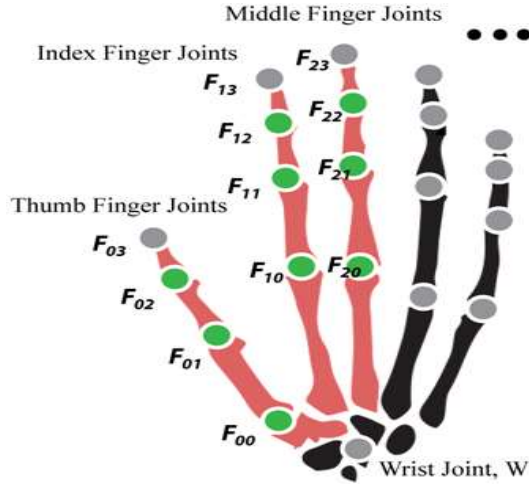


Figure 8. Hand Skeleton.

Circle shapes are joint position that could be detected[29]. Green circles in red bones are angles for using classifying grasping action.

For learning data, we recorded two different hand poses (grasping and non-grasping) and movements. For the cClass 1, various movements maintaining a grasping pose were recorded. And moreover, various movements maintaining a non-grasping pose, such as with the outstretched palm, were recorded for the cClass 2. Therefore, we labeled the two groups of grasping and non-grasping. In addition, we adapted LDA. The objective function to find the optimum projection vector w is shown below (Equation 7 and 8):

$$L(w) = \frac{w^T S_B w}{w^T S_w w} \quad \dots\dots\dots \text{Equation (7)}$$

$$S_w = S_1 + S_2 \quad , \quad S_B = (\mu_1 - \mu_2)(\mu_1 - \mu_2)^T \quad \dots\dots \text{Equation (8)}$$

S_B is the between-class scatter matrix. And S_W is the within-class scatter matrix. S_i is the covariant matrix of θ set in Class i . Moreover, μ_i is mean vector of θ set in Class i . The objective is to find w while minimizing the projected covariance and the projected distance between the classes. Thus, by $\nabla_w L(w) = 0$ and the generalized eigenvalue problem, the optimal projection vector is

$$w^* = S_w^{-1}(\mu_1 - \mu_2) \quad \dots \text{Equation (9)}$$

$$\begin{cases} w^T \theta - b > 0, & \text{class 1} \\ w^T \theta - b < 0, & \text{class 2} \end{cases}, (b = w^T(\mu_1 + \mu_2)/2)$$

The learning accuracy is 95%, and the testing result is 92%. The recognition rate of the pinch gesture of Threegear Systems is about 60% in the same data. Our method shows a higher accuracy result. The real-time recognition rate applied to the VBBT is about 90%.

3-4. Subjects

Inclusion criteria were as follows: (1) unilateral hemiparesis in the upper extremity caused by unilateral first-ever stroke; (2) age ranging from 20–80 years old; (3) no previous disease affecting the function of the hemiparetic arm, except for the stroke itself; (4) free of cognitive, language, visuospatial, and attention deficits that would prevent subjects from following the experimental procedures; and (5) free of medical conditions that would require intensive medical care. Patients were recruited from Jan 2014 to April 2014. The subjects were inpatients and outpatients with stroke from the

Department of Rehabilitation Medicine of a tertiary hospital. One physiatrist affiliated with the department screened the patients, and nine patients who met the above-mentioned criteria and provided their written consent were enrolled in this study. The Seoul National University Bundang Hospital Institutional Review Board approved this study, and it complied with the rules set forth by the Declaration of Helsinki.

3-5. Experimental design

Patients were asked to perform the BBT or the VBBT. The order of the two tests was randomized. Patients took a five-minute rest period between the two tests. The BBT was performed according to previously published instructions[30]. Briefly, patients were instructed to move as many blocks as possible, one at a time, from one compartment to the other for a period of 60 seconds after a 15-second trial period. We instructed patients to perform the VBBT as quickly as possible. The total number of blocks moved to the opposite compartment appropriately was counted. The test of the hemiplegic side followed the test of the normal side. The VBBT was performed using a similar procedure to the BBT, except we used our developed virtual system and a longer familiarization period than the BBT. Patients were seated in front of our system displaying the VBBT environment. In the familiarization session, they were instructed to move the blocks in the virtual environment to the opposite compartment until they thought they were sufficiently familiarized, but they were given a maximum period of 30 minutes. Then, the real one-minute test was performed on the normal side followed by the hemiplegic side. The total number of blocks moved was also counted.

For the baseline assessment, the Fugl–Meyer assessment, Brunnstrom stage in the hemiplegic arm and hand, Korean version of the National Institutes of Health Stroke Scale (K-NIHSS), and the Korean version of the Mini-Mental Status Examination (K-MMSE) were assessed.

3-6. Statistical analysis

To determine the correlation between the number of boxes moved in the BBT and that in the VBBT for each side, and the correlation between the percent ratios [(number of boxes moved by hemiplegic side)/(number of boxes moved by normal side) * 100%] in the BBT and those in the VBBT, Pearson's correlation coefficient for the normally distributed variables or Spearman's rank-correlation coefficient was used. Correlations between 0 and 0.25 were considered low, those between 0.25 and 0.5 were considered fair, those between 0.5 and 0.75 were considered moderate, and those greater than 0.75 were considered strong. A paired t-test was used to test the differences between the number of blocks moved in the BBT and that in the VBBT. P-values less than 0.05 were considered statistically significant. Statistical analysis was performed using the PASW statistical package (SPSS version 18.0, SPSS, Chicago, IL, USA).

Experiment 4. Upper extremity functional evaluation by Fugl-Meyer Assessment scoring using depth-sensing camera

4-1. System for recording motion data with Kinect

The Kinect depth-sensing camera was operated with a frame-rate of 30Hz and was positioned in front of each patient. Before the motion was recorded, the therapist entered patient information including recording arm side and the recording assessment item number into the recording program. The therapist activated the recording function using a recording button in the Graphical User Interface (GUI) panel (Figure 9) after instructing the patient concerning the assessment item to capture the patient's response. Data were stored sequentially with time for the UE joint positions comprising 31 variables including time, and positions of the head, shoulder center, shoulder, elbow, wrist and hand. Data was saved in text file format.



Figure 9. Motion data recording program[31].

The recording program includes patients' abbreviation, recording arm side, assessment item number. When pushing the record button and starting a item of Fugl-Meyer assessment, upper extremity skeleton of a patient can be shown in the monitor.

4-2. Data extraction and normalization of Kinect motion data

The recorded joint movement data from each FMA assessment were extracted. For the left arm, as an example, left hand, left wrist, left elbow, left shoulder, shoulder center and head joint position data were extracted. To extract the same features from both arms, the right side data was mirrored to the left side based on a sagittal plane of the patient. Data recorded at the start and end of each motion were clipped by thresholding of the joint distance between

frames. To remove the differences of seating locations and to normalize body size, all joint data were transformed by minus of initial shoulder center and by dividing the summation of each body length (i.e. wrist-elbow, elbow-shoulder and shoulder-shoulder center).

4-3. FMA scoring based on pattern recognition from Kinect data

To predict a FMA score for each assessment item, an artificial neural network (ANN) among various pattern recognition algorithms was adopted. The prediction target of each item score (0, 1 or 2) was evaluated by one therapist. In machine learning and cognitive science, ANNs are statistical learning models inspired by biological neural networks that have become popular in solving various problems in diverse fields. Especially, it has been adopted to solve motion recognition problems in computer vision[32, 33].

To properly classify motion patterns, features must be extracted from the captured motion data, which contains the positional information of every upper limb joint. Angles and distances between two joints (for example, hand-shoulder, hand-head and elbow-head) are computed from the original position data. Normalized jerky data based on jerky motion analysis is also used as an additional feature. In particular, bounding area and variance data for each feature are also used because the range of the motion increases as the FMA score increases.

The extracted features from motion captured data and the corresponding FMA scores that were evaluated by one therapist were used to train the ANN model. Predicting a score for each assessment depends on different features. Dimensionality reduction using principal component analysis (PCA) was

performed to distinguish major features from all existing features. The original feature dimension was about 100 with slight variation from item to item. Reduction to four to 10 dimensions was done for highly associated principle components. Therefore, different numbers of principal components were used to achieve the best accuracy for each assessment item.

Thirteen assessments (26 scores in total) among all UE FMA determinations were predicted. An identical ANN structure (i.e. number of neurons, number of hidden layers and activation functions) was applied to predict a score for all assessments. However, a different number of principal components were selected for each assessment after PCA dimensionality reduction. Thus, the dimensions of input data depended on the assessments.

4-4. Cross validation of FMA prediction models

Experimental data for each assessment was collected from 41 patients. As both normal side and paralyzed side data were collected for each patient, 82 motion data in total were used to train the ANN model. However, the collected score data displayed a skewed distribution for some assessments. Thus, it was not reliable for the validation to merely divide the collected data into training and testing data.

Using conventional validation, such as fixed partitioning the data set, the error of the training set is not useful estimator of model performance and the error of the test data is not reliable in various testing data sets. Therefore, to reduce variability, multiple rounds of cross-validation are performed using different partitions. The validation results are averaged over the rounds and derive a more accurate estimate of model prediction performance. Presently, 8- to 10-

fold cross validations for each FMA item were performed. The k-fold means that the sample is randomly partitioned into k subsamples. One of the subsamples constitutes testing data and others are training data.

4-5. Assessing the degree of jerky motion using Kinect motion data

The evaluation of the movement impairment is based on the integrated squared jerk[34]. The smoothness of motion is one element for patient assessment. Jerk is the change of acceleration, which is the third derivative of position. Because the integrated squared jerk varies with duration and size of the displacement, it was normalized by $length^2/duration^5$ [35]. The squared root was taken to obtain a quantity proportional to the absolute jerk. The equation for normalized jerk is described in the following equation (10):

$$(Normalized\ Jerk) = \sqrt{1/2 \int_{T_1}^{T_2} Jerk^2(t) dt \times duration^5 / length^2} \dots \dots \text{Equation (10)}$$

Jerk(t) is an 18 dimensional vector because patient motion data has 18 variables (six joint x three dimension). Jerk²(t) is two-norm of the jerk vector. Duration is the length of the clipped data. Length is the maximum distance of a position vector (time t) from the initial (time T₁), which is the greatest difference of motion distance from the start of motion. A higher jerky score derived from this method indicates more jerky movement. Jerky scores during the motion for flexion synergy in FMA were used for analysis.

4-6. Subjects

Patients were recruited from December 2013 to February 2015. Patients were eligible for inclusion if they had unilateral hemiplegia caused by ischemic or

hemorrhagic stroke. Patients were excluded if they younger than 18 years of age; had serious medical complications requiring intensive care, such as pneumonia, urinary tract infection, acute coronary syndrome, inability to provide written informed consent and any other conditions that might interfere with participation. All subjects received detailed information about the study and provided written consent. This research protocol was approved by the Seoul National University Bundang Hospital institutional review board and was conducted in accordance with the regulatory standards of Good Clinical Practice and the Declaration of Helsinki (World Medical Association Declaration of Helsinki: Ethical Principles for Medical Research Involving Human Subjects, 2000).

4-7. Experimental design

Patients were seated comfortably in a chair to test UE FMA. Among the 33 items for UE evaluation, 13 were selected for Kinect motion data recording: flexor synergy (shoulder retraction, shoulder elevation, shoulder abduction, shoulder external rotation, elbow flexion, forearm supination), extensor synergy (shoulder adduction and internal rotation, elbow extension, forearm pronation), volitional motion mixing dynamic flexor and extensor synergy (hand to lumbar spine, shoulder flexion 0° to 90°) and volitional movement with little or no synergy dependence (shoulder abduction 0° to 90°, shoulder flexion 90° to 180°). One occupational therapist with two-year experience in the FMA test did the evaluations. Patient motion was recorded simultaneously by Kinect for all 13 items. Kinect motion data was saved as a separate file, which is upper-limb joint data including time. The saved data and FMA scores

were transferred to an engineering department for analysis.

4-8. Statistical analyses

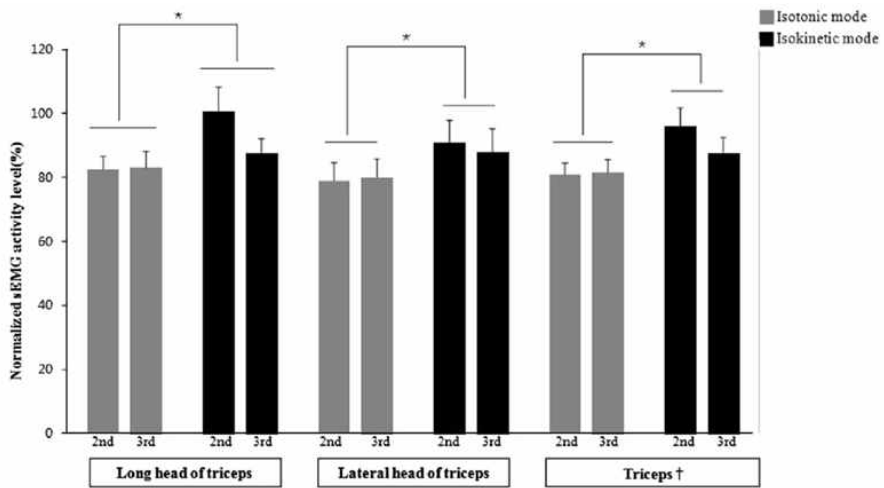
Continuous variables are presented as mean \pm SD for normally distributed data and as median with interquartile range for skewed data. Categorical variables are presented as frequencies (percentages). Prediction accuracies of FMA scores using Kinect for each item were calculated and are represented as a percentage. It was regarded as accurate if FMA score using Kinect was exactly the same as real FMA for each item. The scores of the 13 items for FMA using Kinect and real FMA were summed to assess the correlation. Total score of FMA for selected items ranged from 0 to 26. Pearson's correlation coefficients were calculated to see the correlation between FMA scores using Kinect and real FMA scores in the affected upper extremity for the selected items. In addition, correlation between FMA score using Kinect for selected items and total real FMA score (0-66 points) was investigated using Pearson's correlation coefficient. Log (jerky scores) between hemiplegic and non-hemiplegic side were compared using paired t-test. Correlations between Brunnstrom arm stage and log (jerky score) were investigated using Spearman's correlation coefficient in patients with Brnnstrom arm stage from 3 to 6. Statistical analysis was performed using SPSS version 18.0 (SPSS, Chicago, IL, USA).

RESULTS

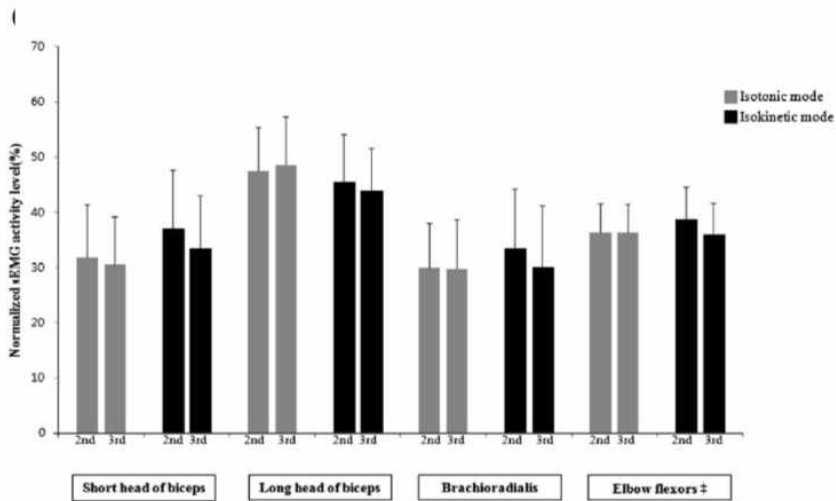
Experiment 1. Electromyographic analysis of upper limb muscles during standardized isotonic and isokinetic robotic exercise

1-1. Surface EMG activity levels according to the mode of exercise

The two-way repeated measures ANOVA revealed significant differences between the modes for the RMS values of the long head of the triceps ($F[1, 8]=7.950$; $P=0.023$), lateral head of the triceps ($F[1, 8]=5.798$; $P=0.043$) and the pooled values from both heads of the triceps ($F[1, 8]=11.168$; $P=0.010$); RMS values for the isokinetic mode were higher (Figure 10A). There were no significant effects of the modes and set orders on the RMS values of the short and long head of the biceps, brachioradialis and pooled values from both heads of the biceps and brachioradialis (Figure 10B).



(A)



(B)

Figure 10. RMS values for elbow extensors (A) and elbow flexors (B) according to the modes of exercise (isotonic vs. isokinetic) and set orders (second and third)[15].

Values are mean \pm SEM. *P < 0.05 for the differences between the mode of exercise with two-way repeated measures ANOVA.

1-2. Analysis of CCI for muscle pairs

Two way repeated measures ANOVA for the CCI from all possible muscle pairs of 8 muscles (total 28 muscle pairs) revealed significant effects of the modes of exercise in only two muscle pairs, the lateral head of the triceps/long head of the biceps ($F[1, 8]=5.988$; $P=0.040$) and the posterior deltoid/lateral head of the triceps ($F[1, 8]=15.152$; $P=0.005$) (Figure 11). There were no significant effects of the set orders and interaction between the modes and set orders on the CCI from these two muscle pairs.

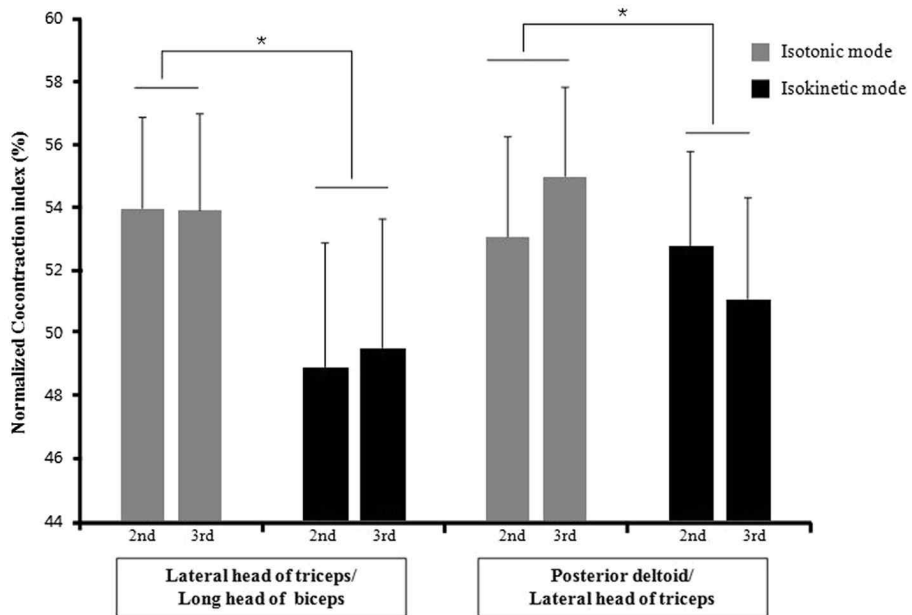


Figure 11. Normalized co-contraction index from the pairs of the lateral head of the triceps/long head of biceps and the posterior deltoid/lateral head of the triceps according to the modes of exercise (isotonic vs. isokinetic) and set orders (second and third)[15].

Values are mean \pm SEM. *P < 0.05 for the differences between the mode of exercise with two-way repeated measures ANOVA.

Experiment 2. Reliability of robotic device assisted modified Tardieu Scale measurements

Stop torque for R1 was 0.59 ± 0.08 for rater 1 and 0.58 ± 0.08 for rater 2. These stop torques were not different between rater 1 and rater 2.

2-1. Test-retest reliability

Test-retest results for the measurements are shown in Table 3. The test-retest reliability was excellent for all measurement methods overall. The reliability of using isokinetic robotic devices showed extremely excellent test-retest reliability.

2-2. Inter-rater reliability

Inter-rater reliability for R2 during passive motion was excellent (Table 4). Although the reliability of R1 during passive motion was also excellent, it was lower than the reliability of R2. R1 measured with isokinetic robotic device showed extremely excellent inter-rater reliability. R1 measured with robotic device without isokinetic motion reduced this reliability. .

Table 3. Test-retest (intra-rater) reliability results for the passive range of motion (R2), angle of catch (R1), Tardieu Scores (R2-R1) data measured with goniometry, isokinetic robotic devices and robotic devices with manual motion.

	Test	Retest	<i>p</i>	SEM	SDD	ICC (1,1) (95% CI)
	Mean (SD)	Mean (SD)				
Angle of catch (R1)						
Rater 1						
Goniometry (shoulder neutral)	119.28 (10.99)	119.28 (13.11)	1.000	4.49	12.44	0.86 (0.66 – 0.94)
Goniometry (90 degree shoulder abduction)	112.89 (12.79)	112.06 (12.58)	0.550	4.03	11.17	0.89 (0.76 – 0.96)
Isokinetic robotic device	114.53 (29.85)	114.93 (28.00)	0.650	2.59	7.18	0.99 (0.98 – 1.00)
Robotic device with manual motion	118.47 (23.69)	122.62 (21.46)	0.117	7.67	21.23	0.89 (0.72 – 0.96)
Rater 2						
Goniometry (shoulder neutral)	118.50 (12.73)	115.83 (15.75)	0.305	7.58	21.01	0.72 (0.40 – 0.88)
Goniometry (90 degree shoulder abduction)	117.28 (14.35)	115.00 (14.59)	0.190	5.12	14.18	0.88 (0.70 – 0.95)
Isokinetic robotic device	113.43 (27.54)	112.96 (28.05)	0.727	3.83	10.62	0.98 (0.95 – 0.99)

Robotic device with manual motion	124.70 (26.99)	124.62 (26.89)	0.958	4.26	11.81	0.98 (0.93 – 0.99)
-----------------------------------	----------------	----------------	-------	------	-------	--------------------

Passive ROM (R2)

Rater 1

Goniometry (shoulder neutral)	163.89 (17.78)	164.94 (16.04)	0.469	4.21	11.67	0.94 (0.85 – 0.98)
-------------------------------	----------------	----------------	-------	------	-------	--------------------

Goniometry (90 degree shoulder abduction)	158.89 (22.66)	157.72 (24.60)	0.391	5.65	15.66	0.94 (0.86 – 0.98)
---	----------------	----------------	-------	------	-------	--------------------

Rater 2

Goniometry (shoulder neutral)	167.72 (13.55)	167.50 (14.96)	0.843	3.22	8.93	0.95 (0.87 – 0.98)
-------------------------------	----------------	----------------	-------	------	------	--------------------

Goniometry (90 degree shoulder abduction)	163.56 (18.76)	160.83 (21.81)	0.193	6.14	17.02	0.91 (0.78 – 0.97)
---	----------------	----------------	-------	------	-------	--------------------

Tardieu Score (R2-R1)

Rater 1

Goniometry (shoulder neutral)	44.61 (18.74)	45.67 (18.14)	0.650	6.12	16.96	0.89 (0.69 – 0.95)
-------------------------------	---------------	---------------	-------	------	-------	--------------------

Goniometry (90 degree shoulder abduction)	46.00 (22.35)	45.17 (22.19)	0.714	6.57	18.21	0.91 (0.79 – 0.97)
---	---------------	---------------	-------	------	-------	--------------------

Rater 2

Goniometry (shoulder neutral)	49.22 (17.85)	51.67 (20.30)	0.383	8.16	22.62	0.82 (0.59 – 0.93)
-------------------------------	---------------	---------------	-------	------	-------	--------------------

Goniometry (90 degree shoulder abduction)	46.28 (19.96)	45.83 (20.05)	0.864	7.46	20.67	0.86 (0.67 – 0.95)
---	---------------	---------------	-------	------	-------	--------------------

Table 4. Inter-rater reliability results for the passive range of motion (R2), angle of catch (R1), Tardieu Scores (R2-R1) data measured with goniometry, isokinetic robotic devices and robotic devices with manual motion.

	Rater 1 Mean (SD)	Rater 2 Mean (SD)	<i>p</i>	SEM	ICC (3,1) (95% CI)
Angle of catch (R1)					
Goniometry (shoulder neutral)	119.28 (11.63)	117.17 (13.28)	0.314	6.10	0.761 (0.468 – 0.903)
Goniometry (90 degree shoulder abduction)	112.47 (12.35)	116.14 (14.03)	0.086	6.02	0.792 (0.526 – 0.917)
Isokinetic robotic device	114.73 (28.89)	113.20 (27.65)	0.447	5.92	0.956 (0.887 – 0.983)
Robotic device with manual motion	121.48 (21.71)	117.86 (21.16)	0.242	8.96	0.825 (0.592 – 0.931)
Passive ROM (R2)					
Goniometry (shoulder neutral)	164.42 (16.66)	167.61 (14.08)	0.105	5.60	0.868 (0.683 – 0.949)
Goniometry (90 degree shoulder abduction)	158.06 (23.30)	162.19 (19.98)	0.009	4.22	0.962 (0.901 – 0.986)
Tardieu Score (R2-R1)					
Goniometry (shoulder neutral)	45.14 (17.79)	50.44 (18.21)	0.094	8.96	0.752 (0.451 – 0.899)
Goniometry (90 degree shoulder abduction)	45.58 (21.76)	46.28 (19.96)	0.814	6.52	0.859 (0.751 – 0.761)

Experiment 3. Upper limb function assessment using virtual Box and Block Test (VBBT) in stroke

Nine stroke patients (67.22 ± 8.09 years old, five males and four females) completed the experimental protocol. Baseline characteristics of all patients are summarized in Table 5. All patients could move some blocks in both the BBT and VBBT, but the numbers of blocks moved was significantly less in the VBBT compared to that in the BBT ($p < 0.001$ in both hemiplegic and non-hemiplegic sides) (Table 6).

Table 5. Baseline characteristics of the subjects

Subject number	Age, years	Gender	Stroke onset to test, days	Stroke type	Hemiplegic side	Brunnstrom-stage in the hemiplegic side		FMA in the hemiplegic upper limb	K-MMSE
						Arm	Hand		
1	75	M	24	Ischemic	Right	5	4	59	26
2	65	M	16	Ischemic	Left	5	5	64	17
3	52	F	36	Ischemic	Right	5	5	56	N.A
4	67	M	39	Ischemic	Left	5	5	62	24
5	75	F	15	Ischemic	Right	5	4	42	22
6	73	M	29	Ischemic	Left	6	5	64	23
7	66	F	31	hemorrhagic	Right	5	5	53	20
8	74	F	20	Ischemic	Left	6	5	63	23
9	58	M	13	Ischemic	Left	5	5	55	27

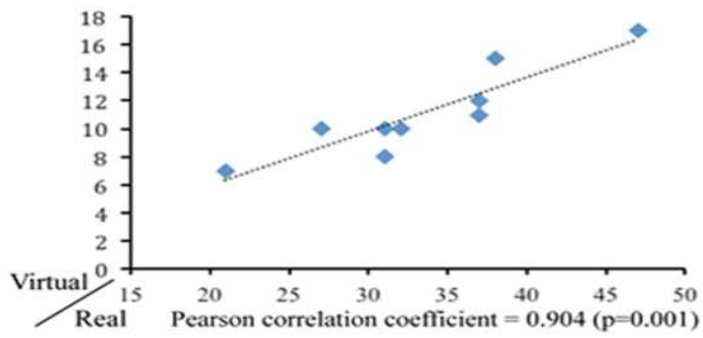
FMA, Fugl-Meyer Assessment; K-MMSE, Korean version of mini-mental status examination

Table 6. Results of the real and virtual box and block test (BBT)

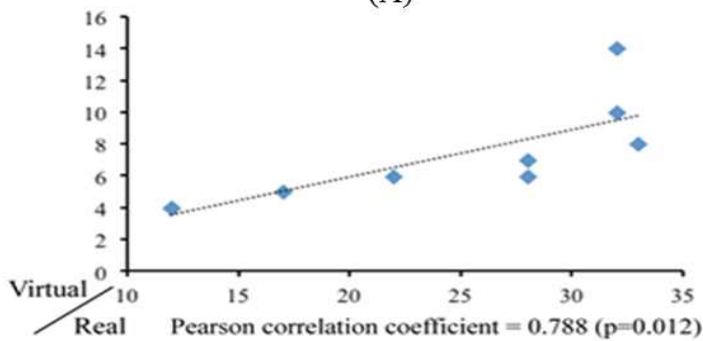
Subject No.	Real BBT		Virtual BBT		% ratio *	
	Hemiplegic side	Non-hemiplegic side	Hemiplegic side	Non-hemiplegic side	Real BBT	Virtual BBT
1	22	37	6	12	59	50
2	28	31	6	8	90	75
3	32	38	14	15	84	93
4	32	37	10	11	86	91
5	12	31	4	10	39	40
6	17	21	5	7	81	71
7	12	27	4	10	44	40
8	28	32	7	10	88	70
9	33	47	8	17	70	47

Values are the number of boxes moved or *% ratio [(the number of boxes moved by the hemiplegic side)/(the number of boxes moved by the normal side) * 100 %].

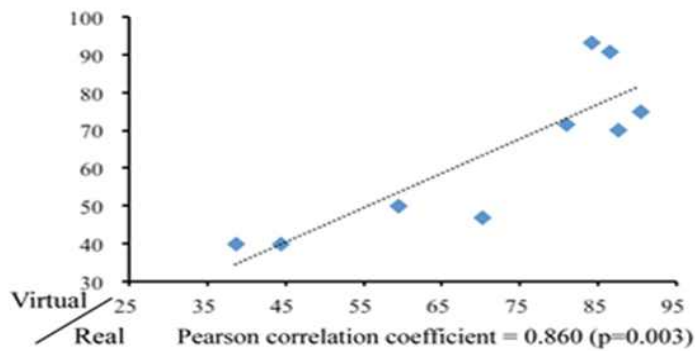
There were strong correlations between the numbers of blocks moved in the BBT and the VBBT in both non-hemiplegic (Pearson's $r = 0.904$, $p = 0.001$) and hemiplegic sides (Pearson's $r = 0.788$, $p = 0.012$) (Figure 12A and 12B). Percent ratios [(number of boxes moved by hemiplegic side)/(number of boxes moved by normal side) * 100 %] in the VBBT also correlated strongly with those in the BBT (Pearson's $r = 0.860$, $p = 0.003$) (Figure 12C).



(A)



(B)



(C)

Figure 12. Correlations between the numbers of box moved in the real and those in the virtual BBT in the non-hemiplegic side (A), and in the hemiplegic side (B), and the correlation between the percent ratios [(the number of boxes moved by the hemiplegic side)/(the number of boxes moved by the normal side) * 100 %] in the real and those in the virtual BBT (C)[29].

Experiment 4. Upper extremity functional evaluation by Fugl-Meyer Assessment scoring using depth-sensing camera

4-1. Characteristics of patients

Among 44 patients who agreed to participate, 41 completed the FMA. The other three patients were not dropped during the FMA but refused to do the test after enrollment. Demographic and clinical characteristics are summarized in Table 7.

Table 7. Baseline characteristics of patients (n=41)

Variables	Results
Age, years ^a	62.6 (12.9)
Sex, no. (%)	
Male	29 (70.7)
Female	12 (29.3)
Time since onset of stroke, days ^b	21 (19)
Paretic side, no.(%)	
Right	15 (36.6)
Left	26 (63.4)
Type of stroke, no.(%)	
Ischemic	28 (68.3)
Hemorrhagic	13 (31.7)
Stroke lesion location	
Cortical	11 (26.8)
Subcortical	30 (73.2)
FMA score in the affected upper extremity ^a	42.5 (19.5)
NIH stroke scale ^b	5 (3)
Brunnstrom stage (arm) ^b	4 (3)
Brunnstrom stage (hand) ^b	4 (4)

FMA-Fugl-Meyer Assessment, NIH-National Institute of Health.

^aMean (SD)

^bMedian (interquartile range)

4-2. Prediction accuracies for FMA scores using Kinect

Prediction accuracies of FMA scores using Kinect for real FMA in the hemiplegic side were above 70% in nine of the 13 selected items (Figure 13). Four items (forearm supination, hand to lumbar spine, shoulder abduction 0° to 90° and shoulder flexion 90° to 180°) showed prediction accuracies between 60% and 70%.

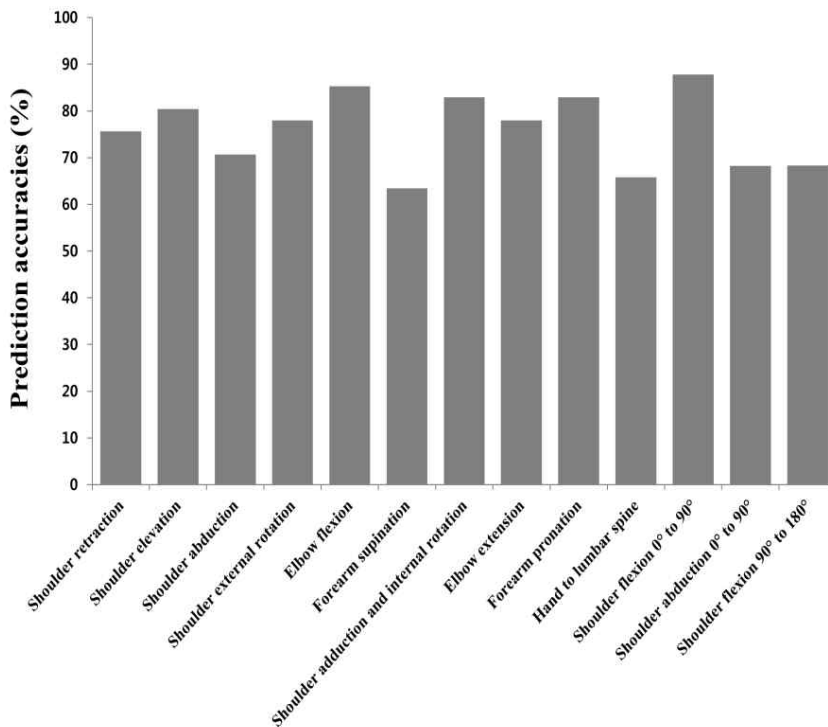
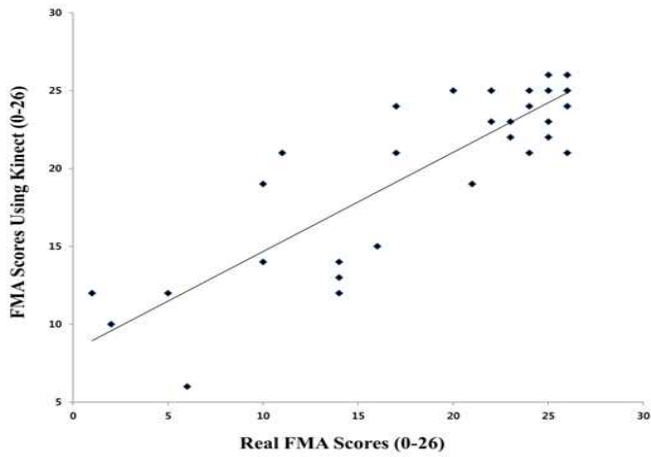


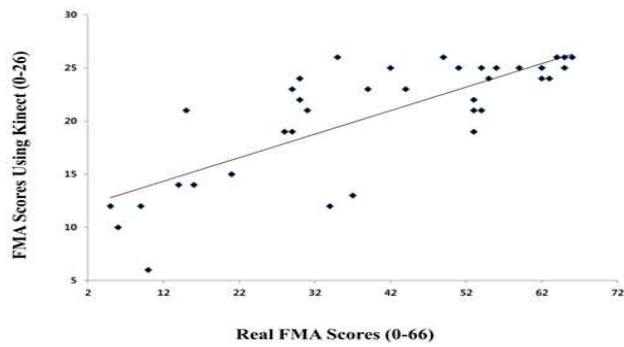
Figure 13. Prediction accuracies(%) of Fugl-Meyer assessment (FMA) scores using Kinect for real FMA scores in each item[31].

4-3. Correlations between FMA scores using Kinect and real scores

Summed predicted FMA scores using Kinect for the 13 selected items showed high correlation with summed real FMA scores for 13 items in hemiplegic UEs (Pearson correlation coefficient=0.873, $P<0.0001$) (Figure 14A). Correlation between summed predicted FMA scores using Kinect for the 13 selected items and summed FMA scores for the 33 items of the hemiplegic UEs were also high (Pearson correlation coefficient=0.799, $P<0.0001$) (Figure 14B).



(A)



(B)

Figure 14. Correlation data[31].

A. Correlation between summed Fugl-Meyer assessment (FMA) using Kinect and real FMA scores for 13 selected items in the hemiplegic upper extremity (Pearson correlation coefficient=0.873, $P<0.0001$). B. Correlation between summed FMA using Kinect for the 13 items and real FMA scores for total of 33 items in the hemiplegic upper extremity (Pearson correlation coefficient=0.799, $P<0.0001$).

4-4. Degree of jerky motion

Jerky scores during flexion synergy motion of FMA calculated from Kinect motion data were log transformed for normalization. Log (jerky score) in the hemiplegic UE was 1.81 ± 0.76 in the hemiplegic arm, which was significantly higher than that in the non-hemiplegic UE (1.21 ± 0.43) ($P < 0.0001$). Log (jerky score) in the hemiplegic UE showed significant negative correlations with Brunnstrom arm stage (Spearman correlation coefficient = -0.387 , $P = 0.046$) in the patients with Brunnstrom arm stage from 3 to 6 ($n = 27$) (Figure 15).

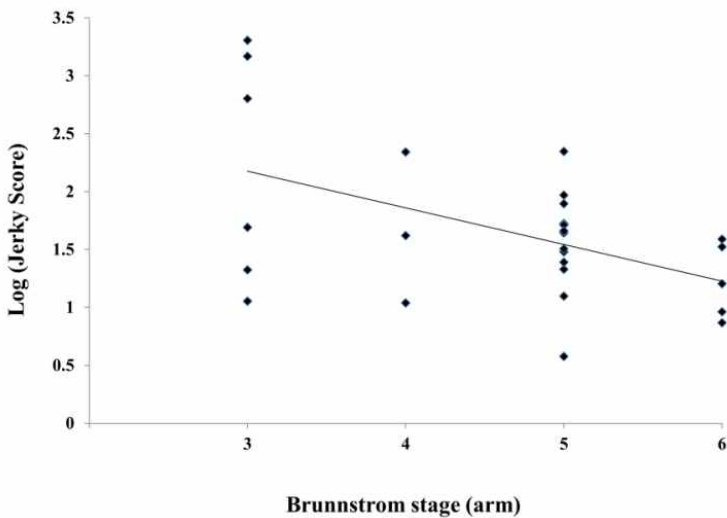


Figure 15. Correlation between log (jerky score) and Brunnstrom arm stage (3 to 6) in the hemiplegic upper extremity ($n = 27$) (Spearman correlation coefficient = -0.387 , $P = 0.046$)[31].

DISCUSSION

In this study, robotic elbow device and virtual reality technologies with a depth-sensing camera were applied to the field of stroke rehabilitation to assess different rehabilitation modalities such as spasticity and function of upper extremity. Specific issues of each experiment are discussed below.

Electromyographic analysis of upper limb muscles during standardized isotonic and isokinetic robotic exercise

In this study to compare the isotonic and isokinetic resistance exercise in the spastic elbow after stroke, the standardized methods for angular velocity and total work realized revealed that the isokinetic mode showed a significantly less number of total repetitions and greater agonist activity during elbow extension than those in the isotonic mode (Figure 10)[15]. In addition, CCI in two muscle pairs were significantly lesser in the isokinetic mode compared to those in the isotonic mode (Figure 11)[15].

The results (greater agonist activity and lesser number of repetitions in isokinetic mode compared to those in isotonic mode) suggest the isokinetic mode makes efficient dynamic muscle action and contributes more to increase motor unit recruitment without applying unnecessary heavy loads[36]. Also these results are compatible with conventional theoretical concept. Theoretically, it has been thought that isokinetic contraction works better than isotonic contraction because the isokinetic mode can induce maximal loading

to muscles through the overall ROM in contrast to the isotonic mode which can load only at the weakest mechanical points during motion[37-39].

However, the previous two studies revealed that agonist activity was greater in isotonic mode than that in isokinetic mode [36, 38]. Remaud[16] argued that these two studies did not standardize the exercise modes. However, after using the standardization method which is similar with that of our study[40], they also reported that agonist muscles activity was greater in the isotonic mode than that in isokinetic mode and the number of repetitions was same in the two modes.

These different results may be caused by different methods used to realize the isotonic mode between the study of Remaud and ours. According to Remaud[16], the isotonic exercise mode described in the study of Remaud is explained as it has threshold resistance and its moving velocity is directly proportional to surplus force. This can be expressed by following equation (11):

$$T_{\text{Human}} - T_{\text{Threshold}} = \Delta T = \begin{cases} K \cdot \omega & (\Delta T > 0) \\ 0 & (\Delta T \leq 0) \end{cases} \quad \dots \text{Equation (11)}$$

where T_{Human} is a force that a subject generates, $T_{\text{Threshold}}$ is a threshold resistance force, K is a proportional constant and ω is angular velocity. Although this isotonic mode simulates actual isotonic exercise by producing various velocities along the force, it is hard to say the isotonic mode is an actual isotonic exercise. The ideal isotonic exercise mode should produce constant resistive force on the muscle regardless of motion. However, the resistive force of the isotonic mode used in the study of Remaud is a function

of the angular velocity (Equation (12)) which means that it is hard to impose constant resistive force to subjects and the experiment conditions cannot be regulated well.

$$T_{\text{Resistive}} = T_{\text{Human}} = T_{\text{Threshold}} + K \cdot \omega \quad (\Delta T > 0 \quad \dots \text{Equation (12)})$$

To solve this problem, isotonic exercise mode of our study was implemented with torque control, inertia compensation and a robot with high back drivability to make the resistive force constant.

It is a usual phenomenon that the co-contraction of antagonist muscles is exaggerated during recovery after stroke, and this may be associated with increased velocity-dependent stretch reflexes, called spasticity[41, 42]. Because stretch reflexes have been known to be proportionally increased to the level of muscular pre-activation[43, 44], strengthening exercises would increase the stretch reflex. From the concept of classical neurodevelopmental treatment, an increase in stretch reflexes or synergy has been thought to be something to be avoided[45].

The experiment results show that co-contraction during elbow extensions is less severe in the isokinetic mode than that in the isotonic mode (Figure 11). The degree of stretch reflex is known to be associated with stretch velocities and joint angle[46]. However the velocities and joint angle between the isotonic and isokinetic modes are controlled, these two parameters cannot explain the differences in the CCI. One possible explanation is that the presence of acceleration during the isotonic mode, which is minimal during isokinetic motion, due to faster and more irregular acceleration, resulting in more increased stretch reflexes[47-49].

Cortical damage after stroke induces cortical overlap of shoulder and elbow

joint representations which results in flexion or extension synergies during voluntary motion[50]. Because preloading increases the synergies, strengthening exercises are expected to increase the synergies during training[51]. However the CCI results show that co-contraction of posterior deltoid and lateral head of the triceps, the component of extension synergy in stroke patients[52], is less severe in isokinetic elbow extension. Because flexion synergy is related with stretch reflexes during elbow extension[46], the larger stretch reflexes during isotonic elbow extension was expected due to faster and more irregular acceleration can lead to more increased flexion synergy. However, there were no differences in CCI of the muscle pairs associated with flexion synergy between the two modes. The reason why isotonic elbow extension induced more extension synergies than the isokinetic mode is difficult to explain at this point in time.

The initial target of elbow extension angle was from 60 to 110 degree, but the range had to be adjusted in several patients because they could not perform isotonic elbow extension fully within this range although they could do in the isokinetic. Patients cannot extend the elbow further if they cannot generate extension torque more than the preset load in the isotonic mode, which is different from the isokinetic mode. The terminal range had to be reduced in patients who needed adjustment of the ROM in isotonic elbow extension (Table 1). ROM limitation may be due to reduced torque generation and stability in the terminal range of extension[16, 54].

This study has several limitations to be considered. First, healthy controls were not included. Therefore, it is hard to conclude that the results of this study are examples of the unique phenomena that occur in stroke patients.

However, because there has been concern about increased abnormal spasticity and synergy during strengthening exercises in the field of stroke rehabilitation, and no studies comparing the different modes of strengthening exercises in stroke patients have been published up to date, this study can give implications for selecting appropriate modes of strengthening and for designing a longitudinal study to investigate the effects of different modes of strengthening in stroke rehabilitation.

Second, the order of two strengthening exercises was not randomized. Because the isotonic exercise always preceded the isokinetic exercise to standardize two exercise modes, this can affect the results of our study due to fatigue. However, resting intervals between the two exercise modes are sufficient in reference to the previous study[16], the Borg scale which indicates muscle fatigue[21] was not different between the two modes after completing each exercise, and the only one patient complained of mild pain (score of 2 in numeric rating scale) after the isotonic exercise, but it was transient.

Finally, because the sample size is small, it is possible that the power to detect the small differences of CCI between the two modes is not sufficient. In addition, it is inconvenient by not performing subgroup analysis according to the different degrees of spasticity.

Reliability of robotic device assisted modified Tardieu Scale measurements

One of the commonly used measurements for spasticity is modified Tardieu scale[55]. However, the reliability of this scale is a concern of previous

studies [56-58]. Therefore, it is important to improve the reliability of measurement for the catch angle. Poor reliability of MTS might be due to the following three possible reasons. First, the measurement of the angle using goniometry manually might have errors. Second, manual motion with fast speed between tests and raters might be different. Third, the feeling of the catch between raters might be different. To guarantee the reliability of MTS and overcome these problems, more experienced raters are needed. However, measurements between experienced raters might still be different. Therefore, in the second series of this study, robotic isokinetic device was applied to overcome these problems. Inter-rater and intra-rater reliability measured by ICC were above 0.95, demonstrating extremely excellent reliability. This reliability was superior to the reliability measured manually or by robotic device without isokinetic motion. Therefore, standardization of fast movement for modified Tardieu scale might be important to increase its reliability. However, our experiment has a limitation, because it is possible that the catch angle during isokinetic fast movement only represents the passive component of spasticity[59]. Increase in velocity during passive motion itself could increase the resistive torque without an active component. In other previous studies, the angle at maximal deceleration has been used[60, 61]. However, the robotic device in our study could not detect this point because it forced the arm to move at a constant velocity regardless of the resistance. One solution for this problem is by finding the angle at maximal torque increase during isokinetic motion. However, our robotic device might have missed this point due to the gap between the teeth of two gears. Surface EMG signals from biceps and triceps muscles were also recorded. However, the onset was too

different between trials to achieve good reliability. In addition, there is a chance of low stretch reflex during isokinetic movement compared to manual movement[62]. Therefore, further development of our robotic device to simulate the manual motion for modified Tardieu Scale and catch the angle at increased resistive torque is required.

Upper limb function assessment using virtual Box and Block Test (VBBT) in stroke

In this third series of study, virtual reality technologies using a depth-sensing camera was applied to measure the upper extremity function. VBBT shows high correlation with the real BBT (Figure 12)[29]. However, VBBT scores were lower than BBT scores for all users (Table 6)[29]. This has some basis in the interaction with the virtual reality. The lack of a device is an important element that affects the convenience of the interaction and the usage in virtual reality. However, these elements result in rather inaccurate input compared to the real environment because of the lack of physical feedback. In addition, the perception of the depth might be difficult with 2D visual feedback alone. Another limitation is the difficulty with ensuring a recognizable grasping posture. Although our grasping detection method detected the grasping motion well using finger joint angles, situations exist in which the depth camera does not see those fingers. Therefore, there is limited recognition of the gestures of users compared to a BBT in which various grasping gestures are used. Although the user must pay attention to the gesture to ensure the grasping motion is recognized, our results show that the assessment of patients in

virtual reality could be trusted.

Regarding virtual tasks, the results from the normal side of stroke patients with relatively intact cognitive functioning and no hemispatial neglect were significantly different even though we provided sufficient time for adaptation. In a pilot trial with healthy subjects, we also found some differences in the results between the tests. This means that the virtual task itself may be fundamentally different from the real test. The real differences might be caused by the absence of sensory input (e.g., weight, texture, and pressure), and we plan to investigate if the addition of sensory input using haptic devices could change the results of the virtual task. The size of the box and the positioning of the box also might have contributed to the differences (especially for the number of boxes moved), but we think the effect on the degree of correlation between the two tests is minimal.

Hardware factors and abnormal hand motion in stroke patients should also be considered. Compared to the normal side, the correlations between the number of boxes moved in the real and virtual BBTs in the hemiplegic side were weaker. We think the main reason for this difference was our system's inability to finely detect the many abnormal motions in stroke patients, such as abnormal synergy patterns or spasticity. Other participant factors, such as preexisting familiarity with the virtual environment, can be considered, but we gave sufficient adaptation time to minimize this effect. Interestingly, the number of boxes moved with the non-hemiplegic side in the real test was about three times that in the VBBT.

The VBBT could be the foundation of a convenient assessment or rehabilitation tool in the home as well as the hospital. The problem with the

virtual program for patients is the accessibility. Patients or their caregivers control programs or sessions by themselves. Using the keyboard, mouse, or other hardware could give them difficulties. For unsupervised assessment and rehabilitation, patients have to be able to control some functions (e.g., execution, end, next level) easily. A voice command system could be a solution. Users can control many smart devices such as smartphones, computers, and even cars using voice commands. The Microsoft Kinect sensor has a multi-microphone and SDK for voice recognition in English. For further virtual rehabilitation programs, use of voice command and recognition system will be more convenient for patients. Furthermore, using the voice commands could help improve stroke patients' impaired language capabilities.

Upper extremity functional evaluation by Fugl-Meyer Assessment scoring using depth-sensing camera

In this experiment with hemiplegic stroke patients, predicted FMA scores using Kinect were highly correlated with real FMA scores (Figure 14)[31]. In addition, jerky scores calculated from Kinect motion data can assess the degree of motion smoothness quantitatively (Figure 15), which could not be provided by conventional FMA with observations[31].

A few tools in the virtual environment to assess the motor impairment after stroke have been investigated in several prior studies, but the correlations with conventional assessment tools were modest (correlation coefficient: 0.53 – 0.66)[63-65]. One study evaluated the activities of daily living (ADL) in the virtual environment and compared it with the scores of Wolf Motor Function

Test (WMFT)[63]. Because WMFT is assessed during actual manipulation of objects, recognition of object's size, weight and texture and sensory feedback is important but the virtual ADL assessment tool using Kinect cannot give this haptic feedback[63]. This limitation may be associated with a modest correlation; an additional device and expense will be required to overcome this limitation. Although two studies using manipulating devices with virtual realities showed modest correlations with conventional assessment tool, additional costs and space are required[64, 65]. In this context, FMA is the best assessment tool which can be predicted using motion tracking with Kinect. Kinect is a relatively inexpensive depth-sensing camera and no additional space and devices are required. The purchase cost continues to decrease and camera performance continues to increase. FMA scoring using Kinect has potential as valid assessment tool for motor function after stroke in the home-based rehabilitation setting.

FMA is valid and is widely used for motor function assessment in stroke patients. But, many items place a time burden on the assessor and patients. In this context, there have been efforts to reduce the FMA item; one study suggested reducing the items for UE evaluation to six[66]. Because of the limitation of Kinect to track various UE motions, only 13 FMA items were presently included. The correlation was high between summed FMA scores using Kinect and real FMA scores for the 13 selected items. Although correlation between summed FMA scores using Kinect and real FMA scores for all 33 UE hemiplegic items was reduced, the correlation coefficient of 0.799 was still high. This indicates that the number of items used in FMA using Kinect could feasibly be decreased, which would decrease the burden

on patients and caregivers during assessment.

Coordinated movement is impaired after stroke; motions are not smooth but rather become jerky. Traditional Brunnstrom recovery phase reveals the recovery of coordinated movement and emergence from synergistic movements[67]. Quantitative measurement of movement smoothness using a robotic device has revealed improvement during the recovery after stroke[68]. Jerky scores using Kinect in our study were well negatively correlated with Brunnstrom stage. This quantitative measure can be used for follow-up of changes in movement in a manner that equivalent in quality to robotic devices but less expensive.

The FMA scoring system using only one Kinect in this study does have some limitations. One is the occlusion of the body part during tracking by Kinect. For instance, Kinect could not track the hand when it is moved to the lumbar spine for FMA. One of the solutions for the occlusion problem is using multiple Kinect Sensors, but this may be associated with increased cost. Wearable sensors such as smart watches or wrist bands providing positional information can also be applied to solve the occlusion problem in our system. Another limitation is that the Kinect Software Development Kit is not appropriate for hand tracking of FMA motion, because it is unable to track pronation/supination, radial/ulnar direction and hand grasp below the wrist during full-body tracking. Some other FMA scores that could not be predicted in this research are required to detect the above hand information with accurate hand position tracking. The items in FMA showing low prediction accuracy are forearm supination, shoulder abduction 0° to 90° and shoulder flexion 90° to 180° , which require the information on forearm rotation. If the

resolution for the hand during full-body tracking with Kinect is increased in the future, the prediction accuracy for items including information on forearm rotation are expected to improve and the FMA items excluded in this study can be added. While waiting for a more advanced form of Kinect, another solution is fusion with other hand tracking sensor, such as the Leap Motion device (Leap Motion, USA), which allows precise hand tracking using a hand point cloud below the wrist. We plan to use Leap Motion for precise hand tracking, and add more items of UE FMA.

More and varied movement data of each assessment item would increase the precision of the FMA system score using Kinect. Imbalance of real FMA scores decreases the prediction accuracies of each item. Techniques explored to solve the imbalance issues include re-sample techniques[69], adaptive training algorithms[70], particle swarm optimization[71] and parameter searching. We used re-sample techniques and cross-validation to minimize errors from dataset imbalance. However, the best way to solve this problem is to gather the more patient data. Although we used the data from 41 stroke patients with various motor impairments, decrease of the imbalance by collecting more data sets and adoption of the above techniques could help increase prediction accuracies. In further work, web-based uploading system of FMA Kinect motion data and real FMA data in various areas could help acquire more patient data. Furthermore, use of a cloud computing system with machine learning ability, such as Microsoft Azure ML, Amazon Machine Learning or IBM Watson Analytics, will facilitate develop of a prediction model capable of self-learning whenever new patient data is uploaded, and to predict FMA score using the model in the absence of a specialist. In our study,

the recording of FMA using Kinect was conducted in the hospital with the supervision of a therapist. Further study to validate the usefulness of advanced system in the real home-setting is required.

CONCLUSION

We investigated the usefulness of robotic and virtual reality technologies for assessment during stroke rehabilitation. Robotic elbow device is found to be useful for comparing different modes of rehabilitation exercises by standardizing specific parameters. Catch angle could be measured reliably with the robotic device. Virtual reality technology using a depth-sensing camera has the potential to be a useful and inexpensive tele-assessment tool to measure post-stroke motor function in a home-based setting. This assessment system with virtual reality could also provide additional quantitative measures for assessing motor function. Assessments tools in our study have some limitations. Further efforts are needed to increase the fidelity of rehabilitation care by combining different current technologies or developing new technologies.

REFERENCES

1. Adamson J, Beswick A, Ebrahim S. Is stroke the most common cause of disability? *Journal of Stroke and Cerebrovascular Diseases*. 2004;13(4):171-7.
2. Lloyd-Jones D, Adams RJ, Brown TM, Carnethon M, Dai S, De Simone G, Ferguson TB, Ford E, Furie K, Gillespie C. Heart disease and stroke statistics—2010 update A report from the American Heart Association. *Circulation*. 2010;121(7):e46-e215.
3. Control CfD, Prevention. Outpatient rehabilitation among stroke survivors--21 States and the District of Columbia, 2005. *MMWR Morbidity and mortality weekly report*. 2007;56(20):504.
4. Brainin M, Teuschl Y, Kalra L. Acute treatment and long-term management of stroke in developing countries. *The Lancet Neurology*. 2007;6(6):553-61.
5. Molinari M, Esquenazi A, Anastasi AA, Nielsen RK, Stoller O, D'Andrea A, Calatayud MB. Rehabilitation Technologies Application in Stroke and Traumatic Brain Injury Patients. *Emerging Therapies in Neurorehabilitation II*: Springer; 2016. p. 29-64.
6. Saposnik G. Virtual Reality in Stroke Rehabilitation. *Ischemic Stroke Therapeutics*: Springer; 2016. p. 225-33.
7. Mehrholz J, Pohl M, Platz T, Kugler J, Elsner B. Electromechanical and robot-assisted arm training for improving activities of daily living, arm

function, and arm muscle strength after stroke. The Cochrane database of systematic reviews. 2015;11:CD006876.

8. Mehrholz J, Elsner B, Werner C, Kugler J, Pohl M. Electromechanical-assisted training for walking after stroke. The Cochrane database of systematic reviews. 2013;7:CD006185.

9. Mostafavi SM, Mousavi P, Dukelow SP, Scott SH. Robot-based assessment of motor and proprioceptive function identifies biomarkers for prediction of functional independence measures. *Journal of neuroengineering and rehabilitation*. 2015;12(1):1.

10. Hussain A, Dailey W, Hughes C, Budhota A, Gamage KC, Vishwanath DA, Kuah C, Chua K, Burdet E, Campolo D, editors. Quantitative motor assessment of upperlimb after unilateral stroke: A preliminary feasibility study with H-Man, a planar robot. *Rehabilitation Robotics (ICORR), 2015 IEEE International Conference on*; 2015: IEEE.

11. Krebs HI, Krams M, Agrafiotis DK, DiBernardo A, Chavez JC, Littman GS, Yang E, Byttebier G, Dipietro L, Rykman A. Robotic measurement of arm movements after stroke establishes biomarkers of motor recovery. *Stroke*. 2014;45(1):200-4.

12. Zhang Z. Microsoft kinect sensor and its effect. *MultiMedia, IEEE*. 2012;19(2):4-10.

13. Gabel M, Gilad-Bachrach R, Renshaw E, Schuster A, editors. Full body gait analysis with Kinect. *Engineering in Medicine and Biology Society (EMBC), 2012 Annual International Conference of the IEEE*; 2012: IEEE.

14. Kurillo G, Chen A, Bajcsy R, Han JJ. Evaluation of upper extremity reachable workspace using Kinect camera. *Technology and health care*:

official journal of the European Society for Engineering and Medicine. 2012;21(6):641-56.

15. Sin M, Kim WS, Park D, Min YS, Kim WJ, Cho K, Paik NJ. Electromyographic analysis of upper limb muscles during standardized isotonic and isokinetic robotic exercise of spastic elbow in patients with stroke. *Journal of electromyography and kinesiology : official journal of the International Society of Electrophysiological Kinesiology*. 2014;24(1):11-7.

16. Remaud A, Cornu C, Guével A. Agonist muscle activity and antagonist muscle co-activity levels during standardized isotonic and isokinetic knee extensions. *Journal of Electromyography and Kinesiology*. 2009;19(3):449-58.

17. Hermens HJ, Freriks B, Disselhorst-Klug C, Rau G. Development of recommendations for SEMG sensors and sensor placement procedures. *Journal of Electromyography and Kinesiology*. 2000;10(5):361-74.

18. Hurst HT, Swarén M, Hébert-Losier K, Ericsson F, Sinclair J, Atkins S, Holmberg H-C. Influence of course type on upper body muscle activity in elite cross-country and downhill mountain bikers during off road downhill cycling. *Journal of Science and Cycling*. 2012;1(1):2-9.

19. Koo TK, Mak AF, Hung L, Dewald JP. Joint position dependence of weakness during maximum isometric voluntary contractions in subjects with hemiparesis. *Arch Phys Med Rehabil*. 2003;84(9):1380-6.

20. Hu X, Tong KY, Song R, Tsang VS, Leung PO, Li L. Variation of muscle coactivation patterns in chronic stroke during robot-assisted elbow training. *Arch Phys Med Rehabil*. 2007;88(8):1022-9.

21. Oberg T, Sandsjo L, Kadefors R. Subjective and objective evaluation of shoulder muscle fatigue. *Ergonomics*. 1994;37(8):1323-33.
22. Breivik H, Borchgrevink PC, Allen SM, Rosseland LA, Romundstad L, Hals EK, Kvarstein G, Stubhaug A. Assessment of pain. *British journal of anaesthesia*. 2008;101(1):17-24.
23. Frost G, Dowling J, Dyson K, Bar-Or O. Cocontraction in three age groups of children during treadmill locomotion. *Journal of electromyography and kinesiology : official journal of the International Society of Electrophysiological Kinesiology*. 1997;7(3):179-86.
24. Falconer K, Winter DA. Quantitative assessment of co-contraction at the ankle joint in walking. *Electromyogr Clin Neurophysiol*. 1985;25(2-3):135-49.
25. Kellis E, Arabatzi F, Papadopoulos C. Muscle co-activation around the knee in drop jumping using the co-contraction index. *Journal of Electromyography and Kinesiology*. 2003;13(3):229-38.
26. Boyd R, Graham H, editors. Conservative options in the management of spasticity in children with cerebral palsy. *Proceedings of 8th EACD meeting*; 1996.
27. Scholtes VA, Becher JG, Beelen A, Lankhorst GJ. Clinical assessment of spasticity in children with cerebral palsy: a critical review of available instruments. *Developmental Medicine & Child Neurology*. 2006;48(1):64-73.
28. Fleiss JL. *Design and analysis of clinical experiments*: John Wiley & Sons; 2011.

29. Cho S, Kim WS, Paik NJ, Bang H. Upper-Limb Function Assessment Using VBBTs for Stroke Patients. *IEEE computer graphics and applications*. 2016;36(1):70-8.
30. Desrosiers J, Bravo G, Hébert R, Dutil E, Mercier L. Validation of the Box and Block Test as a measure of dexterity of elderly people: reliability, validity, and norms studies. *Archives of physical medicine and rehabilitation*. 1994;75(7):751-5.
31. Kim WS, Cho S, Baek D, Bang H, Paik NJ. Upper Extremity Functional Evaluation by Fugl-Meyer Assessment Scoring Using Depth-Sensing Camera in Hemiplegic Stroke Patients. *PloS one*. 2016;11(7):e0158640.
32. Hui Y, Guangmin S, Wenzing S. Human motion recognition based on neural network. *Digital Object Identifier*. 2005;27(2):979-82.
33. Barton G, Lisboa P, Lees A, Attfield S. Gait quality assessment using self-organising artificial neural networks. *Gait & posture*. 2007;25(3):374-9.
34. Teulings H-L, Contreras-Vidal JL, Stelmach GE, Adler CH. Parkinsonism reduces coordination of fingers, wrist, and arm in fine motor control. *Experimental neurology*. 1997;146(1):159-70.
35. Caimmi M, Carda S, Giovanzana C, Maini ES, Sabatini AM, Smania N, Molteni F. Using kinematic analysis to evaluate constraint-induced movement therapy in chronic stroke patients. *Neurorehabilitation and Neural Repair*. 2008;22(1):31-9.

36. Purkayastha S, Cramer JT, Trowbridge CA, Fincher AL, Marek SM. Surface electromyographic amplitude-to-work ratios during isokinetic and isotonic muscle actions. *Journal of athletic training*. 2006;41(3):314-20.
37. Kovalski JE, Heitman RH, Trundle TL, Gilley WF. Isotonic preload versus isokinetic knee extension resistance training. *Medicine and science in sports and exercise*. 1995;27(6):895-9.
38. Schmitz RJ, Westwood KC. Knee Extensor Electromyographic Activity-to-Work Ratio is Greater With Isotonic Than Isokinetic Contractions. *Journal of athletic training*. 2001;36(4):384-7.
39. Smith MJ, Melton P. Isokinetic versus isotonic variable-resistance training. *The American journal of sports medicine*. 1981;9(4):275-9.
40. Remaud A, Cornu C, Guevel A. A methodologic approach for the comparison between dynamic contractions: influences on the neuromuscular system. *J Athl Train*. 2005;40(4):281-7.
41. Frisoli A, Procopio C, Chisari C, Creatini I, Bonfiglio L, Bergamasco M, Rossi B, Carboncini MC. Positive effects of robotic exoskeleton training of upper limb reaching movements after stroke. *Journal of neuroengineering and rehabilitation*. 2012;9:36.
42. Marciniak C. Poststroke hypertonicity: upper limb assessment and treatment. *Topics in stroke rehabilitation*. 2011;18(3):179-94.
43. Lin FM, Sabbahi M. Correlation of spasticity with hyperactive stretch reflexes and motor dysfunction in hemiplegia. *Arch Phys Med Rehabil*. 1999;80(5):526-30.

44. Smeets JB, Erkelens CJ. Dependence of autogenic and heterogenic stretch reflexes on pre-load activity in the human arm. *The Journal of physiology*. 1991;440:455-65.
45. Bobath B. *Adult Hemiplegia: Evaluation and Treatment*. Oxford, UK: Butterworth-Heinemann; 2000.
46. McPherson JG, Stienen AH, Drogos JM, Dewald JP. The relationship between the flexion synergy and stretch reflexes in individuals with chronic hemiparetic stroke. *IEEE International Conference on Rehabilitation Robotics : [proceedings]*. 2011;2011:5975516.
47. Perot C, Mora I, Goubel F. Muscle stretch used as conditioning stimulus for assessing a reciprocal inhibition. *Electromyogr Clin Neurophysiol*. 1992;32(7-8):331-9.
48. Berardelli A, Sabra AF, Hallett M, Berenberg W, Simon SR. Stretch reflexes of triceps surae in patients with upper motor neuron syndromes. *Journal of neurology, neurosurgery, and psychiatry*. 1983;46(1):54-60.
49. Burke D, Hagbarth KE, Lofstedt L. Muscle spindle activity in man during shortening and lengthening contractions. *The Journal of physiology*. 1978;277:131-42.
50. Yao J, Chen A, Carmona C, Dewald JP. Cortical overlap of joint representations contributes to the loss of independent joint control following stroke. *NeuroImage*. 2009;45(2):490-9.
51. Miller LC, Dewald JP. Involuntary paretic wrist/finger flexion forces and EMG increase with shoulder abduction load in individuals with chronic stroke. *Clinical neurophysiology : official journal of the International Federation of Clinical Neurophysiology*. 2012;123(6):1216-25.

52. Brunnstrom S. Movement therapy in hemiplegia. A neurophysiological approach. New York: Harper & Row; 1970.
53. Hunter SM, Hammett L, Ball S, Smith N, Anderson C, Clark A, Tallis R, Rudd A, Pomeroy VM. Dose-response study of mobilisation and tactile stimulation therapy for the upper extremity early after stroke: a phase I trial. *Neurorehabil Neural Repair*. 2011;25(4):314-22.
54. Trumbower RD, Krutky MA, Yang BS, Perreault EJ. Use of self-selected postures to regulate multi-joint stiffness during unconstrained tasks. *PloS one*. 2009;4(5):e5411.
55. Haugh A, Pandyan A, Johnson G. A systematic review of the Tardieu Scale for the measurement of spasticity. *Disability and rehabilitation*. 2006;28(15):899-907.
56. Mackey AH, Walt SE, Lobb G, Stott NS. Intraobserver reliability of the modified Tardieu scale in the upper limb of children with hemiplegia. *Developmental Medicine & Child Neurology*. 2004;46(4):267-72.
57. Yam WKL, Leung MSM. Interrater reliability of Modified Ashworth Scale and Modified Tardieu Scale in children with spastic cerebral palsy. *Journal of child neurology*. 2006;21(12):1031-5.
58. Ansari NN, Naghdi S, Hasson S, Rastgoo M, Amini M, Forogh B. Clinical assessment of ankle plantarflexor spasticity in adult patients after stroke: inter-and intra-rater reliability of the Modified Tardieu Scale. *Brain injury*. 2013;27(5):605-12.
59. Chung SG, Van Rey E, Bai Z, Rymer WZ, Roth EJ, Zhang L-Q. Separate quantification of reflex and nonreflex components of spastic

hypertonia in chronic hemiparesis. Archives of physical medicine and rehabilitation. 2008;89(4):700-10.

60. Lynn B-O, Erwin A, Guy M, Herman B, Davide M, Ellen J, Anne C, Kaat D. Comprehensive quantification of the spastic catch in children with cerebral palsy. Research in developmental disabilities. 2013;34(1):386-96.

61. Paulis WD, Horemans HL, Brouwer BS, Stam HJ. Excellent test-retest and inter-rater reliability for Tardieu Scale measurements with inertial sensors in elbow flexors of stroke patients. Gait & posture. 2011;33(2):185-9.

62. Rabita G, Dupont L, Thevenon A, Linsel-Corbeil G, Pérot C, Vanvelcenaher J. Differences in kinematic parameters and plantarflexor reflex responses between manual (Ashworth) and isokinetic mobilisations in spasticity assessment. Clinical Neurophysiology. 2005;116(1):93-100.

63. Adams RJ, Lichter MD, Krepkovich ET, Ellington A, White M, Diamond PT. Assessing upper extremity motor function in practice of virtual activities of daily living. Neural Systems and Rehabilitation Engineering, IEEE Transactions on. 2015;23(2):287-96.

64. Kowalczewski J, Ravid E, Prochazka A, editors. Fully-automated test of upper-extremity function. Engineering in Medicine and Biology Society, EMBC, 2011 Annual International Conference of the IEEE; 2011: IEEE.

65. Lambercy O, Fluet M-C, Lamers I, Kerkhofs L, Feys P, Gassert R, editors. Assessment of upper limb motor function in patients with multiple sclerosis using the Virtual Peg Insertion Test: A pilot study. Rehabilitation Robotics (ICORR), 2013 IEEE International Conference on; 2013: IEEE.

66. Hsieh Y-W, Hsueh I-P, Chou Y-T, Sheu C-F, Hsieh C-L, Kwakkel G. Development and validation of a short form of the Fugl-Meyer motor scale in patients with stroke. *Stroke*. 2007;38(11):3052-4.
67. Fluet M-C, Lambercy O, Gassert R, editors. Upper limb assessment using a virtual peg insertion test. *Rehabilitation Robotics (ICORR)*, 2011 IEEE International Conference on; 2011: IEEE.
68. Rohrer B, Fasoli S, Krebs HI, Hughes R, Volpe B, Frontera WR, Stein J, Hogan N. Movement smoothness changes during stroke recovery. *The Journal of Neuroscience*. 2002;22(18):8297-304.
69. Lu Y, Guo H, Feldkamp L, editors. Robust neural learning from unbalanced data samples. *Neural Networks Proceedings, 1998 IEEE World Congress on Computational Intelligence The 1998 IEEE International Joint Conference on*; 1998: IEEE.
70. Nguyen GH, Bouzerdoun A, Phung SL, editors. A supervised learning approach for imbalanced data sets. *Pattern Recognition, 2008 ICPR 2008 19th International Conference on*; 2008: IEEE.
71. Adam A, Shapiai I, Ibrahim Z, Khalid M, Chew LC, Jau LW, Watada J, editors. A Modified Artificial Neural Network Learning Algorithm for Imbalanced Data Set Problem. *Computational Intelligence, Communication Systems and Networks (CICSyN)*, 2010 Second International Conference on; 2010: IEEE.

국문 초록

서론: 뇌졸중은 전 세계적으로 장애를 유발하는 주 원인질환 중 하나이다. 뇌졸중 후 회복은 기능적 독립의 가능성을 높이고, 사회경제적 부담을 줄이는데 중요하며 이에 뇌졸중 기능회복을 돕는 재활은 뇌졸중 관리에 있어서 필수적인 요소로 여겨지고 있다. 뇌졸중 재활의 많은 요소 중 평가는 그에 기반한 개별화된 재활치료 계획을 수립하고 치료의 효과를 모니터링 하는데 중요하지만 기존 재활 평가 도구들은 신뢰도와 타당도를 확보하기 위해 지속적인 교육이 필요하며, 정량화된 평가가 어려운 단점이 있다. 최근 로봇 및 가상현실 기술의 재활분야 이용이 증가하고 있으며, 정량적인 평가 및 원격 평가에의 이용이 가능해 기존 재활평가 도구의 단점 극복을 위한 가능성을 보여주고 있다. 하지만 실제 재활환경에서 뇌졸중 환자에게 적용된 기존연구는 미흡한 실정이다. 따라서 본 연구에서는 로봇 및 가상현실 기술을 이용한 뇌졸중 재활 평가 도구를 개발하고 그 임상적 유용성에 대해 알아보고자 하였다.

방법: 본 연구는 4 개의 실험으로 구성되었다. 첫 실험에서는 등장성과 등속성 주관절 신전 운동의 차이를 주관절 로봇을 이용해 평가하고자 하였다. 9 명의 뇌졸중 환자가 최대 등척성 토크의 30%의

저항에 대해 등장성 주관절 신전운동을 총 3 세트 시행하였고, 이후 총 3 세트의 등속적 주관절 신전운동을 시행하였다. 한 연구대상에서 대응되는 등장성 및 등속적 주관절 신전운동은 평균 각속도 및 총 일량 (total work amount)이 같도록 표준화 되었다. 운동시 편마비측 어깨와 주관절 근육에 표면 근전도를 부착해 신호를 얻었고, 표준화된 제곱근 평균 (normalized root mean square, RMS)과 동시수축지수 (co-contraction index, CCI)를 계산해 분석에 이용하였다.

두번째 실험에서는 경직측정 도구인 modified Tardieu Sclae (MTS)의 신뢰도를 주관절 로봇을 이용해 높이기 위한 시도를 하였다. 독립된 두 명의 평가자가 기존의 MTS를 각각 세번씩 평가하였고, 이후 주관절 로봇을 이용해 200도의 각속도로 등속도 움직임시 접힘각도 (catch angle)를 측정하였다. 평가자가 직접 시행할 때와 주관절 로봇을 이용할 때의 MTS의 평가자 내 및 평가자간 신뢰도를 분석하였다.

세번째 실험에서는 상지기능 평가에 이용되는 Box and Block Test (BBT)를 가상현실 환경에서 깊이인식 카메라 (depth-sensing camera)를 이용해 구현하였다. Virtual BBT (VBBT)를 경증 뇌졸중 환자에게 적용하여 타당도를 평가하였다.

네번째 실험에서는 깊이인식 카메라를 이용해 Fugl-Meyer Assessment (FMA)를 예측 평가하는 시스템을 개발하였다. 이를 위해 41 명의 편마비를 가진 뇌졸중 환자가 참여하였다. FMA의 총 33개 항목 중 깊이인식 카메라를 이용한 예측 시스템을 위해 13개의 항목이 선정되었다. 한명의 작업치료사가 FMA를 평가할 때 동시에 깊이인식 카메라를 이용해 환자의 동작을 녹화하고 데이터를 저장하였다. 저장된 모션 데이터에 주성분분석 (principal component analysis)를 통한 차원감소 (dimensionality reduction) 및 신경망학습을 적용해 실제 FMA 점수를 예측하는 알고리즘을 생성하였다. 동시에 불규칙한(jerky) 움직임을 정량화하기 위해 jerky score를 생성해 내는 알고리즘도 개발하였다. FMA의 각 항목의 예측 정확도와 실제 FMA 점수와의 상관성을 분석하였다.

결과: 뇌졸중 후 경직성 편마비를 가진 환자에서는 등속성 저항운동이 등장성 저항운동에 비해 효과적으로 작용근을 훈련시킬 수 있었고 (삼두박근의 표준화된 RMS: 등속성, 96.0 ± 17.0 (2nd), 87.8 ± 14.4 (3rd)/등장성, 80.9 ± 11.0 (2nd), 81.6 ± 12.4 (3rd), $F[1,8] = 11.168$; $P = 0.010$), 경직 및 비정상 협응을 의미하는 동시 수축도 더 적음을 확인할 수 있었다. 또한 주관절 로봇의 등속성 움직임을

통한 접힘각도 측정은 기존 수동적 방법에 비해 높은 평가자내, 평가자간 신뢰도를 보였다.

BBT 및 VBBT 시 환자가 옮긴 박스의 수는 마비측과 정상측 모두에서 높은 상관관계를 보여주었다 (마비측: Pearson' s r =0.788, $P=0.012$ / 정상측: Pearson' s r =0.904, $P=0.001$). 깊이인식 카메라를 이용한 FMA 예측 점수는 각 항목별로 65%에서 87%사이의 정확도를 보였으며, 9 개의 항목에서는 70% 이상의 정확도를 확인할 수 있었다. 깊이인식 카메라를 이용해 평가한 13 개 항목의 FMA 의 총합은 해당하는 13 개 항목의 치료사 평가 점수의 합과 높은 상관관계를 보였으며 (Pearson' s r=0.873, $P<0.0001$), 33 개 항목의 치료사 평가 점수의 합과도 높은 상관관계를 유지하였다 (Pearson' s correlation coefficient=0.799, $P<0.0001$). 로그변환된 jerky score 는 마비측 (1.81 ± 0.76) 에서 정상측 (1.21 ± 0.43)에 비해 높은 점수를 보였으며, Brunnstrom 단계와는 유의한 음의 상관관계를 보였다 (Spearman correlation coefficient= -0.387, $P=0.046$).

결론: 주관절 로봇은 서로 다른 재활치료 기법을 보다 표준화된 방법으로 비교하는데 유용하게 사용될 수 있으며, 기존 평가 방법의

신뢰도를 높일 수 있었다. 깊이인식 카메라를 이용한 가상현실 기술은 뇌졸중 후 재가재활환경에서 운동 기능을 평가할 수 있는 유용하고 비용효과적인 평가도구를 제공할 수 있으며, 기존의 평가도구와 비교해 추가적으로 정량화된 움직임의 평가가 가능하였다. 따라서 본 연구를 통해 로봇 및 가상현실 기술이 뇌졸중 재활 평가를 위해 유용하게 이용될 수 있음을 확인할 수 있었다. 하지만 본 연구에서의 평가도구들은 개선되어야 할 한계점 들을 가지고 있고, 향후 기존기술의 병합 및 고도화를 통해 한계를 극복하기 위한 노력이 필요할 것이다. 이러한 노력은 향후 재활평가에서의 정확도, 타당도를 높이고 좀더 풍부한 임상정보를 제공해 줄 수 있을 것으로 기대된다.

주요어 : 로봇, 가상현실, 편마비, 뇌졸중, 깊이인식 카메라, 평가, 재활

학 번 : 2012-30491

Disclosure for copyright

Contents for experiment 1 were from the following reference: “Sin M, Kim WS, Park D, Min YS, Kim WJ, Cho K, Paik NJ. Electromyographic analysis of upper limb muscles during standardized isotonic and isokinetic robotic exercise of spastic elbow in patients with stroke. *Journal of electromyography and kinesiology : official journal of the International Society of Electrophysiological Kinesiology*. 2014;24(1):11-7”. Copyright for reuse of whole contents was permitted from Elsevier. The license terms and conditions for this agreement can be found in the supplementary page.

Contents for experiment 3 were from the following reference: “Cho S, Kim WS, Paik NJ, Bang H. Upper-Limb Function Assessment Using VBBTs for Stroke Patients. *IEEE computer graphics and applications*. 2016;36(1):70-8”. Copyright for reuse of whole contents was permitted from IEEE. The license terms and conditions for this agreement can be found in the supplementary page. In addition, in reference to IEEE copyrighted material which is used with permission in this thesis, the IEEE does not endorse any of [Seoul National University College of Medicine]'s products or services. Internal or personal use of this material is permitted. If interested in reprinting/republishing IEEE copyrighted material for advertising or promotional purposes or for creating new collective works for resale or redistribution, please go to the following webpage to learn how to obtain a license from RightsLink:

http://www.ieee.org/publications_standards/publications/rights/rights_link.html.

Contents for experiment 4 were from the following reference: “Kim WS, Cho S, Baek D, Bang H, Paik NJ. Upper Extremity Functional Evaluation by Fugl-Meyer Assessment Scoring Using Depth-Sensing Camera in Hemiplegic Stroke Patients. *PloS one*. 2016;11(7):e0158640”. According to policy for content license applied to all of PLOS journals (<http://journals.plos.org/plosone/s/content-license>), the author used the contents with this citation and disclosure.

**ELSEVIER LICENSE
TERMS AND CONDITIONS**

Jul 24, 2016

This Agreement between Won ("You") and Elsevier ("Elsevier") consists of your license details and the terms and conditions provided by Elsevier and Copyright Clearance Center.

License Number	3915360071687
License date	Jul 24, 2016
Licensed Content Publisher	Elsevier
Licensed Content Publication	Journal of Electromyography and Kinesiology
Licensed Content Title	Electromyographic analysis of upper limb muscles during standardized isotonic and isokinetic robotic exercise of spastic elbow in patients with stroke
Licensed Content Author	Minki Sin, Won-Seok Kim, Daegeun Park, Yu-Sun Min, Woo Jin Kim, Kyujin Cho, Nam-Jong Paik
Licensed Content Date	February 2014
Licensed Content Volume Number	24
Licensed Content Issue Number	1
Licensed Content Pages	7
Start Page	11
End Page	17
Type of Use	reuse in a thesis/dissertation
Portion	full article
Format	both print and electronic
Are you the author of this Elsevier article?	Yes
Will you be translating?	No
Order reference number	
Title of your thesis/dissertation	Development and Validation of Assessment Tools Using Robotic and Virtual Reality Technologies in Stroke Rehabilitation
Expected completion date	Aug 2016
Estimated size (number of pages)	80
Elsevier VAT number	GB 494 6272 12
Requestor Location	Won-Seok Kim Department of Rehabilitation Medicine Seoul National Univ. Bundang Hospital 82, Gumi-ro 173 Beon-gil, Bundang-gu Seongnam-si, Gyeonggi-do 463-707 Korea, Republic Of Attn: Won-Seok Kim
Total	0.00 USD
Terms and Conditions	

INTRODUCTION

1. The publisher for this copyrighted material is Elsevier. By clicking "accept" in connection with completing this licensing transaction, you agree that the following terms and conditions apply to this transaction (along with the Billing and Payment terms and conditions established by Copyright Clearance Center, Inc. ("CCC"), at the time that you opened your Rightslink account and that are available at any time at <http://myaccount.copyright.com>).

GENERAL TERMS

2. Elsevier hereby grants you permission to reproduce the aforementioned material subject to the terms and conditions indicated.

3. Acknowledgement: If any part of the material to be used (for example, figures) has appeared in our publication with credit or acknowledgement to another source, permission must also be sought from that source. If such permission is not obtained then that material may not be included in your publication/copies. Suitable acknowledgement to the source must be made, either as a footnote or in a reference list at the end of your publication, as follows:

"Reprinted from Publication title, Vol /edition number, Author(s), Title of article / title of chapter, Pages No., Copyright (Year), with permission from Elsevier [OR APPLICABLE SOCIETY COPYRIGHT OWNER]." Also Lancet special credit - "Reprinted from The Lancet, Vol. number, Author(s), Title of article, Pages No., Copyright (Year), with permission from Elsevier."

4. Reproduction of this material is confined to the purpose and/or media for which permission is hereby given.

5. Altering/Modifying Material: Not Permitted. However figures and illustrations may be altered/adapted minimally to serve your work. Any other abbreviations, additions, deletions and/or any other alterations shall be made only with prior written authorization of Elsevier Ltd. (Please contact Elsevier at permissions@elsevier.com)

6. If the permission fee for the requested use of our material is waived in this instance, please be advised that your future requests for Elsevier materials may attract a fee.

7. **Reservation of Rights:** Publisher reserves all rights not specifically granted in the combination of (i) the license details provided by you and accepted in the course of this licensing transaction, (ii) these terms and conditions and (iii) CCC's Billing and Payment terms and conditions.
8. **License Contingent Upon Payment:** While you may exercise the rights licensed immediately upon issuance of the license at the end of the licensing process for the transaction, provided that you have disclosed complete and accurate details of your proposed use, no license is finally effective unless and until full payment is received from you (either by publisher or by CCC) as provided in CCC's Billing and Payment terms and conditions. If full payment is not received on a timely basis, then any license preliminarily granted shall be deemed automatically revoked and shall be void as if never granted. Further, in the event that you breach any of these terms and conditions or any of CCC's Billing and Payment terms and conditions, the license is automatically revoked and shall be void as if never granted. Use of materials as described in a revoked license, as well as any use of the materials beyond the scope of an unrevoked license, may constitute copyright infringement and publisher reserves the right to take any and all action to protect its copyright in the materials.
9. **Warranties:** Publisher makes no representations or warranties with respect to the licensed material.
10. **Indemnity:** You hereby indemnify and agree to hold harmless publisher and CCC, and their respective officers, directors, employees and agents, from and against any and all claims arising out of your use of the licensed material other than as specifically authorized pursuant to this license.
11. **No Transfer of License:** This license is personal to you and may not be sublicensed, assigned, or transferred by you to any other person without publisher's written permission.
12. **No Amendment Except in Writing:** This license may not be amended except in a writing signed by both parties (or, in the case of publisher, by CCC on publisher's behalf).
13. **Objection to Contrary Terms:** Publisher hereby objects to any terms contained in any purchase order, acknowledgment, check

endorsement or other writing prepared by you, which terms are inconsistent with these terms and conditions or CCC's Billing and Payment terms and conditions. These terms and conditions, together with CCC's Billing and Payment terms and conditions (which are incorporated herein), comprise the entire agreement between you and publisher (and CCC) concerning this licensing transaction. In the event of any conflict between your obligations established by these terms and conditions and those established by CCC's Billing and Payment terms and conditions, these terms and conditions shall control.

14. **Revocation:** Elsevier or Copyright Clearance Center may deny the permissions described in this License at their sole discretion, for any reason or no reason, with a full refund payable to you. Notice of such denial will be made using the contact information provided by you. Failure to receive such notice will not alter or invalidate the denial. In no event will Elsevier or Copyright Clearance Center be responsible or liable for any costs, expenses or damage incurred by you as a result of a denial of your permission request, other than a refund of the amount(s) paid by you to Elsevier and/or Copyright Clearance Center for denied permissions.

LIMITED LICENSE

The following terms and conditions apply only to specific license types:

15. **Translation:** This permission is granted for non-exclusive world **English** rights only unless your license was granted for translation rights. If you licensed translation rights you may only translate this content into the languages you requested. A professional translator must perform all translations and reproduce the content word for word preserving the integrity of the article.

16. **Posting licensed content on any Website:** The following terms and conditions apply as follows: Licensing material from an Elsevier journal: All content posted to the web site must maintain the copyright information line on the bottom of each image; A hyper-text must be included to the Homepage of the journal from which you are licensing at

<http://www.sciencedirect.com/science/journal/xxxxx> or the

Elsevier homepage for books at <http://www.elsevier.com>; Central Storage: This license does not include permission for a scanned version of the material to be stored in a central repository such as that provided by Heron/XanEdu.

Licensing material from an Elsevier book: A hyper-text link must be included to the Elsevier homepage at <http://www.elsevier.com>. All content posted to the web site must maintain the copyright information line on the bottom of each image.

Posting licensed content on Electronic reserve: In addition to the above the following clauses are applicable: The web site must be password-protected and made available only to bona fide students registered on a relevant course. This permission is granted for 1 year only. You may obtain a new license for future website posting.

17. **For journal authors:** the following clauses are applicable in addition to the above:

Preprints:

A preprint is an author's own write-up of research results and analysis, it has not been peer-reviewed, nor has it had any other value added to it by a publisher (such as formatting, copyright, technical enhancement etc.).

Authors can share their preprints anywhere at any time.

Preprints should not be added to or enhanced in any way in order to appear more like, or to substitute for, the final versions of articles however authors can update their preprints on arXiv or RePEc with their Accepted Author Manuscript (see below).

If accepted for publication, we encourage authors to link from the preprint to their formal publication via its DOI. Millions of researchers have access to the formal publications on ScienceDirect, and so links will help users to find, access, cite and use the best available version. Please note that Cell Press, The Lancet and some society-owned have different preprint policies. Information on these policies is available on the journal homepage.

Accepted Author Manuscripts: An accepted author manuscript is the manuscript of an article that has been accepted for publication and which typically includes author-incorporated

changes suggested during submission, peer review and editor-author communications.

Authors can share their accepted author manuscript:

- immediately
 - via their non-commercial person homepage or blog
 - by updating a preprint in arXiv or RePEc with the accepted manuscript
 - via their research institute or institutional repository for internal institutional uses or as part of an invitation-only research collaboration work-group
 - directly by providing copies to their students or to research collaborators for their personal use
 - for private scholarly sharing as part of an invitation-only work group on commercial sites with which Elsevier has an agreement
- after the embargo period
 - via non-commercial hosting platforms such as their institutional repository
 - via commercial sites with which Elsevier has an agreement

In all cases accepted manuscripts should:

- link to the formal publication via its DOI
- bear a CC-BY-NC-ND license - this is easy to do
- if aggregated with other manuscripts, for example in a repository or other site, be shared in alignment with our hosting policy not be added to or enhanced in any way to appear more like, or to substitute for, the published journal article.

Published journal article (JPA): A published journal article (PJA) is the definitive final record of published research that appears or will appear in the journal and embodies all value-adding publishing activities including peer review co-ordination, copy-editing, formatting, (if relevant) pagination and online enrichment.

Policies for sharing publishing journal articles differ for

subscription and gold open access articles:

Subscription Articles: If you are an author, please share a link to your article rather than the full-text. Millions of researchers have access to the formal publications on ScienceDirect, and so links will help your users to find, access, cite, and use the best available version.

Theses and dissertations which contain embedded PJAs as part of the formal submission can be posted publicly by the awarding institution with DOI links back to the formal publications on ScienceDirect.

If you are affiliated with a library that subscribes to ScienceDirect you have additional private sharing rights for others' research accessed under that agreement. This includes use for classroom teaching and internal training at the institution (including use in course packs and courseware programs), and inclusion of the article for grant funding purposes.

Gold Open Access Articles: May be shared according to the author-selected end-user license and should contain a [CrossMark logo](#), the end user license, and a DOI link to the formal publication on ScienceDirect.

Please refer to Elsevier's [posting policy](#) for further information.

18. **For book authors** the following clauses are applicable in addition to the above: Authors are permitted to place a brief summary of their work online only. You are not allowed to download and post the published electronic version of your chapter, nor may you scan the printed edition to create an electronic version. **Posting to a repository:** Authors are permitted to post a summary of their chapter only in their institution's repository.

19. **Thesis/Dissertation:** If your license is for use in a thesis/dissertation your thesis may be submitted to your institution in either print or electronic form. Should your thesis be published commercially, please reapply for permission. These requirements include permission for the Library and Archives of Canada to supply single copies, on demand, of the complete thesis and include permission for Proquest/UMI to supply single copies, on demand, of the complete thesis. Should your thesis be published commercially, please reapply for permission.

Theses and dissertations which contain embedded PJAs as part of the formal submission can be posted publicly by the awarding institution with DOI links back to the formal publications on ScienceDirect.

Elsevier Open Access Terms and Conditions

You can publish open access with Elsevier in hundreds of open access journals or in nearly 2000 established subscription journals that support open access publishing. Permitted third party re-use of these open access articles is defined by the author's choice of Creative Commons user license. See our [open access license policy](#) for more information.

Terms & Conditions applicable to all Open Access articles published with Elsevier:

Any reuse of the article must not represent the author as endorsing the adaptation of the article nor should the article be modified in such a way as to damage the author's honour or reputation. If any changes have been made, such changes must be clearly indicated.

The author(s) must be appropriately credited and we ask that you include the end user license and a DOI link to the formal publication on ScienceDirect.

If any part of the material to be used (for example, figures) has appeared in our publication with credit or acknowledgement to another source it is the responsibility of the user to ensure their reuse complies with the terms and conditions determined by the rights holder.

Additional Terms & Conditions applicable to each Creative Commons user license:

CC BY: The CC-BY license allows users to copy, to create extracts, abstracts and new works from the Article, to alter and revise the Article and to make commercial use of the Article (including reuse and/or resale of the Article by commercial entities), provided the user gives appropriate credit (with a link to the formal publication through the relevant DOI), provides a link to the license, indicates if changes were made and the licensor is not represented as endorsing the use made of the work. The full details of the license are available at

<http://creativecommons.org/licenses/by/4.0>.

CC BY NC SA: The CC BY-NC-SA license allows users to copy, to create extracts, abstracts and new works from the Article, to alter and revise the Article, provided this is not done for commercial purposes, and that the user gives appropriate credit (with a link to the formal publication through the relevant DOI), provides a link to the license, indicates if changes were made and the licensor is not represented as endorsing the use made of the work. Further, any new works must be made available on the same conditions. The full details of the license are available at <http://creativecommons.org/licenses/by-nc-sa/4.0>.

CC BY NC ND: The CC BY-NC-ND license allows users to copy and distribute the Article, provided this is not done for commercial purposes and further does not permit distribution of the Article if it is changed or edited in any way, and provided the user gives appropriate credit (with a link to the formal publication through the relevant DOI), provides a link to the license, and that the licensor is not represented as endorsing the use made of the work. The full details of the license are available at <http://creativecommons.org/licenses/by-nc-nd/4.0>.

Any commercial reuse of Open Access articles published with a CC BY NC SA or CC BY NC ND license requires permission from Elsevier and will be subject to a fee.

Commercial reuse includes:

- Associating advertising with the full text of the Article
- Charging fees for document delivery or access
- Article aggregation
- Systematic distribution via e-mail lists or share buttons

Posting or linking by commercial companies for use by customers of those companies.

20. Other Conditions:

v1.8

Questions? customercare@copyright.com or +1-855-239-3415 (toll free in the US) or +1-978-646-2777.



RightsLink®

[Home](#)
[Create Account](#)
[Help](#)


Title: Upper-Limb Function Assessment Using VBTTs for Stroke Patients

Author: Sungmin Cho; Won-Seok Kim; Nam-Jong Paik; Hyunwoo Bang

Publication: IEEE Computer Graphics and Applications Magazine

Publisher: IEEE

Date: Jan.-Feb. 2016

Copyright © 2016, IEEE

[LOGIN](#)

If you're a copyright.com user, you can login to RightsLink using your copyright.com credentials. Already a **RightsLink user** or want to [learn more?](#)

Thesis / Dissertation Reuse

The IEEE does not require individuals working on a thesis to obtain a formal reuse license, however, you may print out this statement to be used as a permission grant:

Requirements to be followed when using any portion (e.g., figure, graph, table, or textual material) of an IEEE copyrighted paper in a thesis:

- 1) In the case of textual material (e.g., using short quotes or referring to the work within these papers) users must give full credit to the original source (author, paper, publication) followed by the IEEE copyright line © 2011 IEEE.
- 2) In the case of illustrations or tabular material, we require that the copyright line © [Year of original publication] IEEE appear prominently with each reprinted figure and/or table.
- 3) If a substantial portion of the original paper is to be used, and if you are not the senior author, also obtain the senior author's approval.

Requirements to be followed when using an entire IEEE copyrighted paper in a thesis:

- 1) The following IEEE copyright/ credit notice should be placed prominently in the references: © [year of original publication] IEEE. Reprinted, with permission, from [author names, paper title, IEEE publication title, and month/year of publication]
- 2) Only the accepted version of an IEEE copyrighted paper can be used when posting the paper or your thesis on-line.
- 3) In placing the thesis on the author's university website, please display the following message in a prominent place on the website: In reference to IEEE copyrighted material which is used with permission in this thesis, the IEEE does not endorse any of [university/educational entity's name goes here]'s products or services. Internal or personal use of this material is permitted. If interested in reprinting/republishing IEEE copyrighted material for advertising or promotional purposes or for creating new collective works for resale or redistribution, please go to http://www.ieee.org/publications_standards/publications/rights/rights_link.html to learn how to obtain a License from RightsLink.

If applicable, University Microfilms and/or ProQuest Library, or the Archives of Canada may supply single copies of the dissertation.

[BACK](#)
[CLOSE WINDOW](#)

Copyright © 2016 [Copyright Clearance Center, Inc.](#) All Rights Reserved. [Privacy statement.](#) [Terms and Conditions.](#)
Comments? We would like to hear from you. E-mail us at customercare@copyright.com